

YUKON MINERAL EXPLORATION PROGRAM (YMEP) REPORT ON THE WOLF PROPERTY: 2023 ROTARY AIRBLAST DRILLING

Whitehorse Mining District, Yukon

GRANT_NUMBER	CLAIM NAME
YF01861- YF01868	CU 1-CU 8
YD09011- YD09038	FLOW 1- FLOW 28
YD09039- YD09048	FLOW 29- FLOW 38
YD09049- YD09058	FLOW 39- FLOW 48
YD09059- YD09074	FLOW 49- FLOW 64
YD09075- YD09084	FLOW 65- FLOW 74
YD09085- YD09096	FLOW 75- FLOW 86
YD09097- YD09102	FLOW 87- FLOW 92
YD09103-YD09118	FLOW 93- FLOW 108
YD09119- YD09139	FLOW 109- FLOW 129
YD09159	FLOW 130
YD09161- YD09178	FLOW 131-FLOW 148
YD05873- YD05890	WCK 1- WCK 18
YF08941- YF08982	WOLF 1- WOLF 42
YD89953- YD90020	WOLF 43-WOLF 110
YD97071- YD97190	WOLF 111-WOLF 230

Whitehorse Mining District

NTS: 115N01

UTM 540910E 6988950N (NAD83 Zone 7N)

Work Performed Between:

RAB Drilling: June 6th- July 19th, 2023

Written by:

Steven Walsh, M.Sc., G.I.T.

December 15, 2023

Page Intentionally Left Blank

0.0 SUMMARY

The following report documents exploration work completed during the 2023 field season on the Wolf property, which is wholly owned by White Gold Corp. (“WGO” or “White Gold”). The property is located in the Dawson Range area of west-central Yukon, centered at UTM 540910E 6988950N (NAD 83 Zone 7) and is covered by 1:50,000 scale map sheet 115N01. The property is located approximately 120 Km southwest of Dawson City, or alternatively, approximately 30 km southwest of the confluence of the White and Yukon Rivers. The property consists of 404 contiguous quartz claims covering an area of approximately 8,209 hectares. See Table 1 or Appendix III for a complete claims listing.

The collective work of previous field seasons culminated in the generation of the Taurus target, a new drill-ready gold target on the Wolf property. When past gold in soil geochemistry data is interpreted in conjunction with GT Probe, 1st vertical derivative magnetics (“VD1”), and local mapping results, a correlation between all datasets emerges, forming the Taurus target. This correlation suggests gold mineralization is associated with a mapped siliciclastic unit which, in the absence of outcrop, can be identified by a notable low magnetic response (VD1)(Figure 7b). This target has a strike length of at least 1km which made it readily testable with a modest rotary air-blast (“RAB”) drilling program.

In 2023, White Gold returned to the property and conducted a maiden RAB drilling program on the Taurus target. The program, consisting of four RAB holes drilled over eight days, totalling 300.23 m, was designed to test the general tenor of gold mineralization of the Taurus target, along with the possibility of a strong magnetic low as proxy for the Carmacks Siliciclastics. The particulars of the RAB drilling program are presented in Section 5.0 (2023 RAB Drill Program).

RAB drilling produced broad low-grade gold enrichment in holes 001, 002, and 004, with isolated mineralization in hole 003. Drilling confirmed the presence of gold mineralization within oxidized fractures associated with the Carmacks Group Siliciclastic Unit, though the full picture remains unclear regarding the nature of mineralization (RAB001 vs. RAB002), and the involvement of alteration leaving questions to be answered through a diamond drilling program.

Sub-gram per ton silver grades ranging 200-500ppm, with outliers reaching 1200ppm (33.5-35.0m in RAB003) persist throughout all drill holes, see assay certificates in Appendix II.

Highlight results for the 2023 RAB drilling program on the Wolf property include:

- WLFTRS23RAB002:
 - WLFTRS23RAB002 produced the most significant zone with 0.61g/t Au over 10.67m (18.29-28.96m), including 2.51g/t Au over 1.52m (18.29-19.81m), within a broader zone of 0.32g/t Au over 30.47m (13.72-44.19m).
 - Mildly elevated copper levels (55-217ppm Cu) throughout 30.47m gold zone (13.72-44.19m)
- WLFTRS23RAB003:
 - WLFTRS23RAB003 produced the greatest single sample interval outlier of the program with 6.55g/t Au, 37.38ppm Mo over 1.52m (21.34-22.86m) concentrated at the faulted lithological contact between the Carmacks volcanics and underlying diorite (see photo 6). All within a broader zone of 0.81g/t over 15.24m (19.81-35.05m).
 - 1.52m interval of 0.11g/t Au, 623ppm Pb, 584ppm Zn, and 1225ppm Ag at the base of the gold zone (33.53-35.05m)
- WLFTRS23RAB004

- WLFTRS23RAB004 produced the largest continuous zone of gold mineralization with 0.19g/t Au over the entire 70.10m of the hole.
- The sinuous pattern of gold values throughout the length of the hole (elevated at top and bottom, with a substantial dip in the middle regardless of the oxidation of the surrounding lithology supports the theory that mineralization is tied directly to oxidized structures and not blanket oxidized lithological zones.

The nature of RAB drilling, which returns rock chips to the surface, makes it inherently challenging for geologists to log and record rock types accurately or determine any structural data. Therefore, indirect observations must be relied upon. Geochemical analysis, along with discrimination and ternary charts, indicate the primary rock types encountered during drilling consisted of basaltic and andesitic Carmacks volcanics, with noticed variation in the type of magmatic source signature (basaltic andesite to basalt, trachy-andesite to alkali basalt, Figure 20). Most of the RAB samples have geochemical signatures that fall into the field of porphyry prospectivity (Figure 24, Richards et al., 2012).

To accurately determine the effects of alteration and mineralization encountered during the 2023 RAB drilling program, future exploration work must consist of more detailed geological and alteration mapping to assist in vectoring diamond drilling. Results of this program have presented multiple targets for diamond drilling for future exploration, including low-high magnetic interfaces (WLFTRS23RAB004) and the contact between Carmack siliciclastics and basalts (WLFTRS23RAB002). Immediate exploration work, consisting of detailed drill core logging coupled with OTV surveying, should focus on structural controls and alteration controls. Supplemental targeting could be focussed on the search for a gold feeder structure associated with Carmacks siliciclastic emplacements.

Table of Contents

0.0	SUMMARY	3
1.0	Location and Access	8
	Location and Tenure	8
	Access and Infrastructure	12
	Physiography	12
	Climate	12
2.0	GEOLOGY.....	13
	2.1 Regional Geology	13
	2.2 Property Geology	15
	Lithologies	16
	Alteration	16
	Structures.....	17
	Mineralization	17
3.0	PREVIOUS EXPLORATION WORK.....	19
	1970: Quintana Minerals	19
	1971: Astor Mines and Marguerite Lake Mines (JV).....	20
	1994: O. Davis	20
	1998: Shawn Ryan.....	20
	1999: Deltango Gold	20
	2005: Shawn Ryan.....	20
	2008: Shawn Ryan.....	20
	2009: Shawn Ryan.....	20
	2010: Shawn Ryan.....	21
	2011 Ethos	21
	2016: Shawn Ryan.....	21
	2017-Present: White Gold Corp.....	21
4.0	EXPLORATION TARGET	26
	4.1 Targeted Mineralization.....	26
	4.2 Deposit Model.....	26
5.0	2023 EXPLORATION PROGRAM	27
	5.1 Rotary Air Blast Drilling	27
	5.1.1 Procedures	34
	5.1.2 Sample Preparation	36
	5.1.3 Analytical Methodology.....	36

5.1.4 QAQC Program	37
6.0 2023 EXPLORATION RESULTS.....	38
6.1 Rotary Air Blast.....	38
6.1.1 Taurus Target	38
6.1.2 RAB Hole Descriptions	43
7.0 INTERPRETATION AND CONCLUSIONS.....	51
8.0 RECOMENDATIONS	54
9.0 REFERENCES	55
10.0 STATEMENT OF EXPENSES	56
11.0 STATEMENT OF QUALIFICATIONS.....	57

List of Figures

Figure 1. Wolf Property Regional Location map	9
Figure 2. Wolf Property Local Location and Claim Map	10
Figure 3. Terrane map of the northern Cordillera (modified from Nelson et al 2013). The red star is the approximate location of the property.	14
Figure 4. Local Geology of the Wolf Property with Mineral Showings. Modified from Cooley, 2017 and YGS.	18
Figure 5. Compiled Gold in Soil Geochemistry of the Wolf Property	24
Figure 6. Compiled Gold in Soil Geochemistry and GT Probe Sampling	25
Figure 7. Relationships Between Gold in Soil, GT Probe, Magnetics, and Lithology of the Taurus Target.	27
Figure 8. Location of Wolf RAB Drill Collars with drill traces against Au in the soil.....	29
Figure 9. Wolf 2023 RAB Drilling Plotted Against GT Probe, gold in soil, and LiDAR.....	30
Figure 10. Conductivity Profile Across the Taurus Target Showing Proposed Target /Deposit Model and Planned RAB Holes.....	31
Figure 11. 2023 RAB Drilling Plotted Against First Derivative Magnetic, GT Probe, and Gold in Soil.	32
Figure 12. 2023 RAB Holes Plotted Against GT Probe (Au), Gold in Soil, and Lithology. Interpreted Surface Trace of Gold Anomaly and Gold assay values along RAB drill traces also shown	33
Figure 13. RAB drill downhole plot showing gold values vs. depth in meters. X-axis scale independent for each hole.....	39
Figure 14. RAB drill downhole plot showing molybdenum values vs. depth in meters. X-axes independent for each hole.	39
Figure 15. Tukey box and whisker plot showing gold assay results, including far outliers.	40
Figure 16. Tukey box and whisker plot showing gold assay results, excluding outliers.	40
Figure 17. Tukey box and whisker plot showing molybdenum assay results, including outliers.	41
Figure 18. Cross-sections of RAB holes 001 and 002 showing lithology and gold assays in ppm	47
Figure 19. Cross-section of RAB holes 003 and 004 showing lithology paired with gold assays in ppm....	48
Figure 20. Volcanic Rock classification chart using immobile elements as proxy for TAS diagram (Pearce, 1996) showing distribution of the 2023 RAB hole samples.....	49
Figure 21. Modified figure 18 separating gold grade percentiles by colour. Note the preference of the 95 th and 100 th percentile, in red and purple respectively, for the basalt and alkali basalt regions.	50
Figure 22. Alumina Saturation in Igneous Rocks (Barton and Young, 2002)	50

Figure 23. Tectonic classification of mafic igneous rocks showing a distinction between rocks encountered on the Taurus target during the 2023 RAB drilling program.	51
Figure 24. Porphyry prospectivity diagram showing RAB samples which do not plot as Basalt carry a geochemical signature similar to adakite-like rock. Note that adakite-like clusters tend to carry Cu-Au mineralization (Richards et al., 2012)	54

List of Tables

Table 1. Wolf Property Mineral Claims and Expiry Dates	11
Table 2. Wolf Property Notable Gold Correlation Coefficients	26
Table 3. Wolf Property Soil Geochemistry Percentiles of Notable Metals	26
Table 4. Wolf 2023 RAB drill hole collar data	28
Table 5. BV Labs Analytical Methods and Detection Limits for the 2023 Wolf RAB Drilling Program	36
Table 6. 2023 RAB Drilling QA/QC Sample Insertion Summary	37
Table 7. Summary of White Gold QA/QC Submissions for RAB Drilling Program	37
Table 8. Wolf Taurus RAB Drilling Assay Summary	38
Table 9. Correlation table of key elements from 2023 RAB drilling assay results	41
Table 10. Correlation tables for each 2023 RAB hole	42
Table 11. Summary of 2023 RAB Exploration Expenditures	56

List of Photos

Photo 1. Typical Physiography of the Wolf Property	13
Photo 2. Aries Showing. Historical Bulldozer trenches re-vegetated by trees.	19
Photo 3. Typical RAB pad not requiring any ground manipulation or ground disturbance.	34
Photo 4. RAB pad requiring slight ground manipulation.	35
Photo 5. RAB Chip tray for WLFTRS23RAB0010.0-30.5m with oxidized andesite interval (45-75ft).	43
Photo 6. WLFTRS23RAB001 OTV image of oxidized fractures and patchy alteration 6.00-9.65m.....	43
Photo 7. WLFTRS23RAB001 OTV image of oxidized fractures as host of au-mineralization 18.00-21.50m43	
Photo 8. WLFTRS23RAB002 Chips showing mineralized and oxidized intervals (0.0-30.5m).	44
Photo 9. WLFTRS23RAB002 Oxidized Au-bearing fractures within unoxidized Carmacks andesite. Peak assay value of 0.715g/t Au at 24.4-25.9m	44
Photo 10. WLFTRS23RAB002 27.00-30.00m Sharp drop-off in Au mineralization to <0.2g/t occurs as oxidation density increases.....	44
Photo 11. Mineralized Fault within non-oxidized Carmacks andesite. Peak Au value of 6.55g/t Au at 21.34-22.86m.....	45
Photo 12. WLFTRS23RAB003 Chip Trays. Notice the restriction of pervasive oxidation to the upper 10ft (3m), Adding evidence to mineralization be restricted to tight oxidized structures.....	45
Photo 13. WLFTRS23RAB004 Chip Trays. Note the comparison with WLFTRS23RAB003 chip trays in photo 12, which was drilled nearby in the opposite azimuth. Oxidation is significantly widespread, as is the persistent low Au values of 0.19g/t Au over entirety of the hole (0.0-70.10m (0-230ft).	46
Photo 14. WLFTRS23RAB002 OTV Images showing variability of oxidation alteration in relation to mineralization. Note that oxidized structures at 18.00-19.50m (upper left column) are mineralized with 2.51g/t Au where as the more oxidized region at 27.50-30.65m (lower right column) are restricted to < 0.25g/t Au. This suggests that mineralization is tied to the structures and not extensive penetrating oxidation into surrounding wall rock.....	53

1.0 Location and Access

Location and Tenure

The Wolf property is located approximately 120km south of Dawson City in west-central Yukon, centered at UTM 540910E 6988950N (NAD 83 Zone 7) and is covered by 1:50000 scale NTS map sheet 115N01 (Figure 1). More locally, the Wolf property is located approximately 30km southwest of the confluence of the White and Yukon Rivers. The Wolf property is comprised of 404 contiguous claims covering an area of approximately 8,209 hectares. Claim particulars including the tenure names, number, and expiry dates are provided below in Table 1. A local location map is provided in Figure 2.

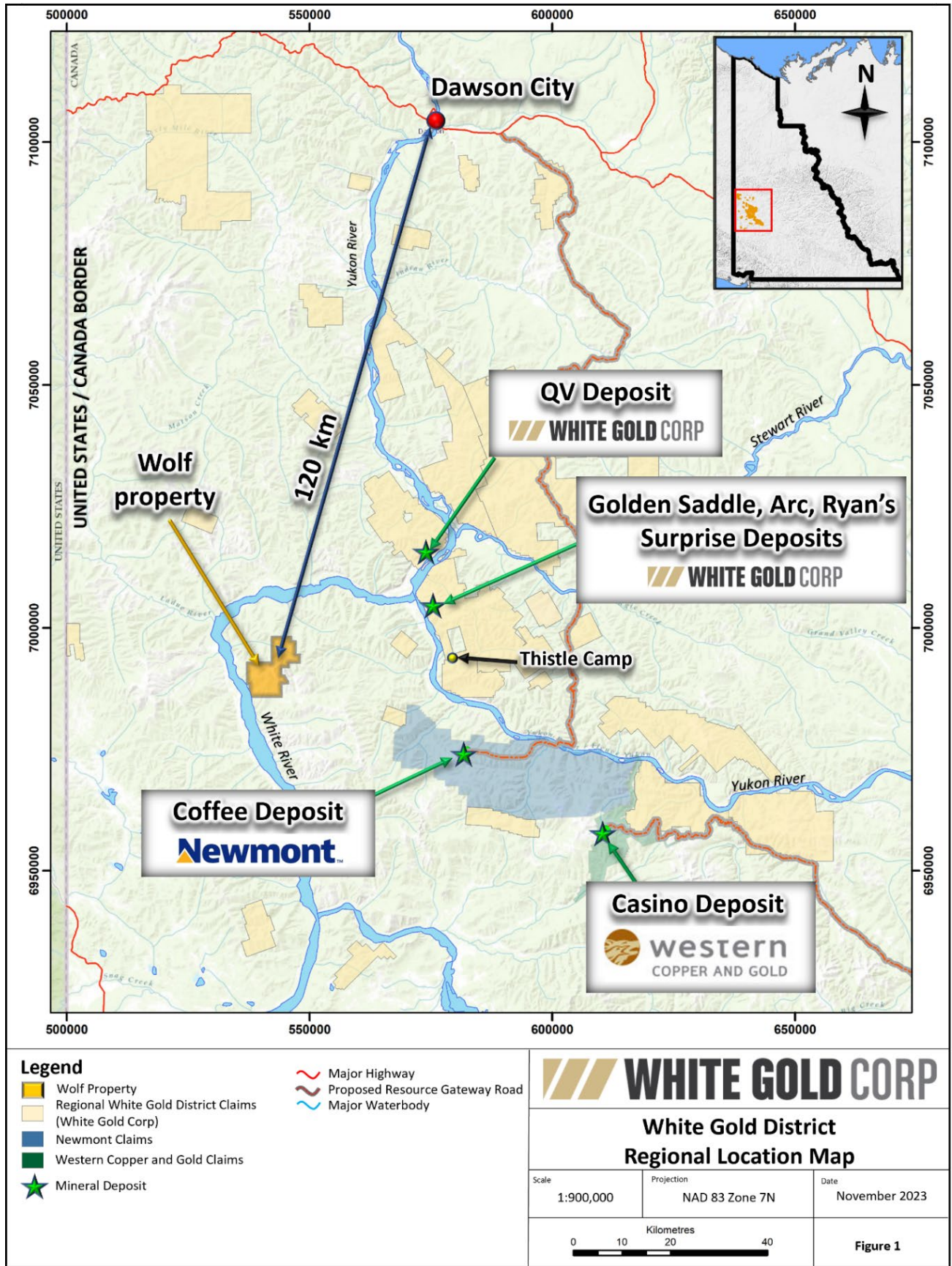


Figure 1. Wolf Property Regional Location map

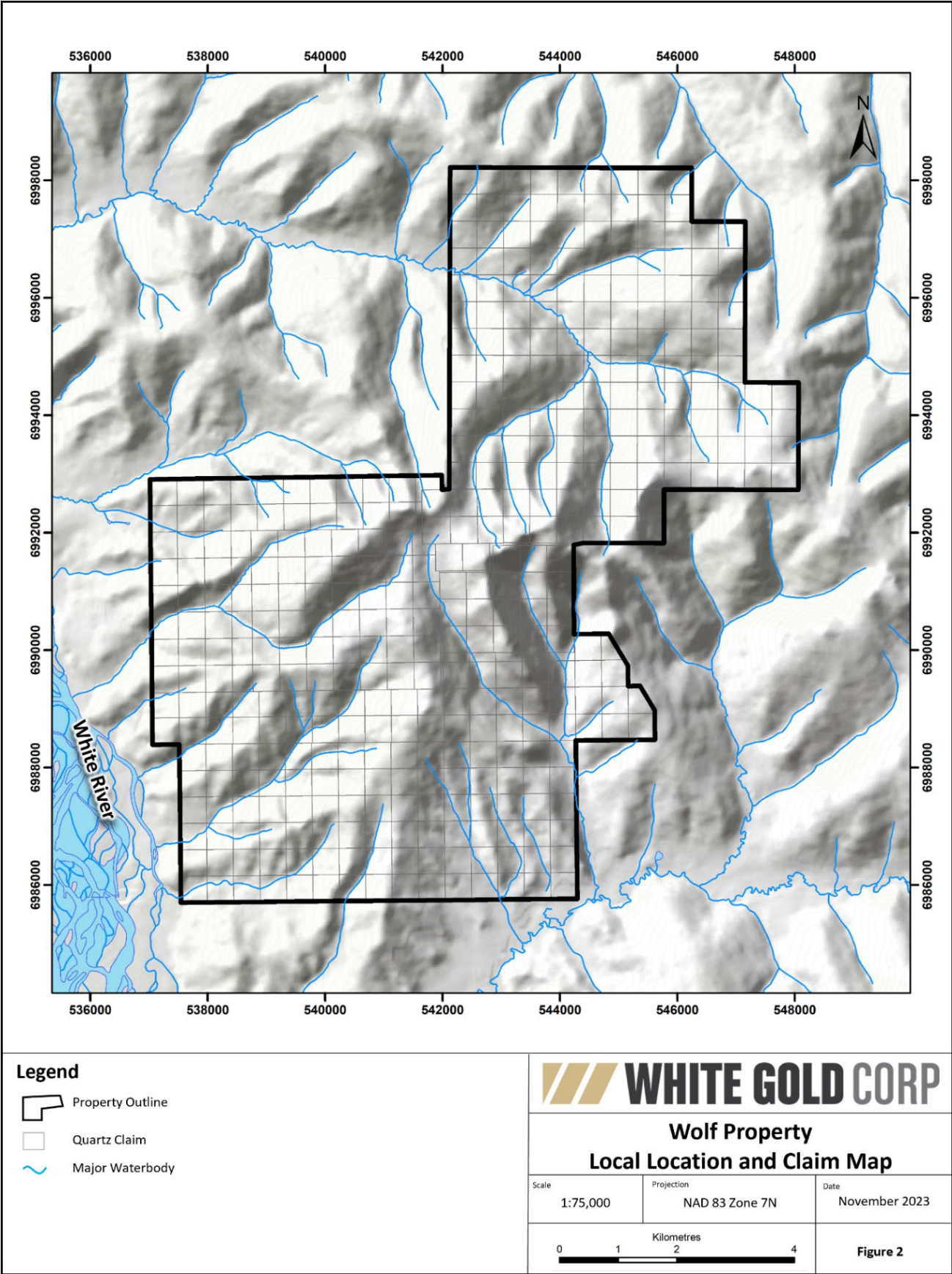


Figure 2. Wolf Property Local Location and Claim Map

Table 1. Wolf Property Mineral Claims and Expiry Dates

GRANT_NUM	TENURE	STATUS	LABEL	# of Claims	OWNER	EXPIRY_DATE
YF01861- YF01868	Quartz	Active	CU 1-CU 8	8	White Gold Corp. - 100%	2025-02-15
YD09011- YD09038	Quartz	Active	FLOW 1- FLOW 28	28	White Gold Corp. - 100%	2025-02-15
YD09039- YD09048	Quartz	Active	FLOW 29- FLOW 38	10	White Gold Corp. - 100%	2024-02-15
YD09049	Quartz	Active	FLOW 39	1	White Gold Corp. - 100%	2024-02-15
YD09050	Quartz	Active	FLOW 40	1	White Gold Corp. - 100%	2025-02-15
YD09051	Quartz	Active	FLOW 41	1	White Gold Corp. - 100%	2024-02-15
YD09052	Quartz	Active	FLOW 42	1	White Gold Corp. - 100%	2025-02-15
YD09053	Quartz	Active	FLOW 43	1	White Gold Corp. - 100%	2024-02-15
YD09054	Quartz	Active	FLOW 44	1	White Gold Corp. - 100%	2025-02-15
YD09055	Quartz	Active	FLOW 45	1	White Gold Corp. - 100%	2024-02-15
YD09056	Quartz	Active	FLOW 46	1	White Gold Corp. - 100%	2025-02-15
YD09057	Quartz	Active	FLOW 47	1	White Gold Corp. - 100%	2024-02-15
YD09058	Quartz	Active	FLOW 48	1	White Gold Corp. - 100%	2025-02-15
YD09059	Quartz	Active	FLOW 49	1	White Gold Corp. - 100%	2024-02-15
YD09060	Quartz	Active	FLOW 50	1	White Gold Corp. - 100%	2025-02-15
YD09061	Quartz	Active	FLOW 51	1	White Gold Corp. - 100%	2024-02-15
YD09062	Quartz	Active	FLOW 52	1	White Gold Corp. - 100%	2025-02-15
YD09063	Quartz	Active	FLOW 53	1	White Gold Corp. - 100%	2024-02-15
YD09064	Quartz	Active	FLOW 54	1	White Gold Corp. - 100%	2025-02-15
YD09065-YD9139	Quartz	Active	FLOW 55- FLOW 129	75	White Gold Corp. - 100%	2024-02-15
YD09159	Quartz	Active	FLOW 130	1	White Gold Corp. - 100%	2024-02-15
YD09161- YD09178	Quartz	Active	FLOW 131-FLOW 148	18	White Gold Corp. - 100%	2024-02-15
YD05873- YD05890	Quartz	Active	WCK 1- WCK 9	9	White Gold Corp. - 100%	2025-02-15
YD05882-YD0584	Quartz	Active	WCK10 – WCK12	3	White Gold Corp. - 100%	2024-02-15
YD05885-YD05890	Quartz	Active	WCK13 – WCK18	6	White Gold Corp. - 100%	2025-02-15
YF08941- YF08953	Quartz	Active	WOLF 1- WOLF 13	13	White Gold Corp. - 100%	2025-02-15
YF08954	Quartz	Active	WOLF 14	1	White Gold Corp. - 100%	2024-02-15
YF08955-YF08982	Quartz	Active	WOLF 15-WOLF 42	28	White Gold Corp. - 100%	2025-02-15
YD89953	Quartz	Active	WOLF 43	1	White Gold Corp. - 100%	2024-02-15
YD89954-YD89976	Quartz	Active	WOLF 44-WOLF 66	23	White Gold Corp. - 100%	2025-02-15
YD89977	Quartz	Active	WOLF 67	1	White Gold Corp. - 100%	2024-02-15
YD89978	Quartz	Active	WOLF 68	1	White Gold Corp. - 100%	2025-02-15
YD89979-YD89983	Quartz	Active	WOLF 69-WOLF 73	5	White Gold Corp. - 100%	2024-02-15
YD89984	Quartz	Active	WOLF 74	1	White Gold Corp. - 100%	2025-02-15
YD89985	Quartz	Active	WOLF 75	1	White Gold Corp. - 100%	2024-02-15
YD89986	Quartz	Active	WOLF 76	1	White Gold Corp. - 100%	2025-02-15
YD89987	Quartz	Active	WOLF 77	1	White Gold Corp. - 100%	2024-02-15
YD89988	Quartz	Active	WOLF 78	1	White Gold Corp. - 100%	2025-02-15
YD89989	Quartz	Active	WOLF 79	1	White Gold Corp. - 100%	2024-02-15
YD89990	Quartz	Active	WOLF 80	1	White Gold Corp. - 100%	2025-02-15
YD89991-YD89998	Quartz	Active	WOLF 81-WOLF 88	8	White Gold Corp. - 100%	2024-02-15
YD89999-YD90007	Quartz	Active	WOLF 89-WOLF 97	9	White Gold Corp. - 100%	2025-02-15
YD90008	Quartz	Active	WOLF 98	1	White Gold Corp. - 100%	2024-02-15
YD90009	Quartz	Active	WOLF 99	1	White Gold Corp. - 100%	2025-02-15
YD90010-YD90020	Quartz	Active	WOLF 100-WOLF 110	11	White Gold Corp. - 100%	2024-02-15
YD97071-YD97072	Quartz	Active	WOLF 111-WOLF 112	2	White Gold Corp. - 100%	2025-02-15
YD97073-YD97100	Quartz	Active	WOLF 113-WOLF 140	28	White Gold Corp. - 100%	2024-02-15
YD97101	Quartz	Active	WOLF 141	1	White Gold Corp. - 100%	2025-02-15
YD97102	Quartz	Active	WOLF 142	1	White Gold Corp. - 100%	2024-02-15
YD97103	Quartz	Active	WOLF 143	1	White Gold Corp. - 100%	2025-02-15
YD97104	Quartz	Active	WOLF 144	1	White Gold Corp. - 100%	2024-02-15
YD97105	Quartz	Active	WOLF 145	1	White Gold Corp. - 100%	2025-02-15
YD97106	Quartz	Active	WOLF 146	1	White Gold Corp. - 100%	2024-02-15

GRANT_NUM	TENURE	STATUS	LABEL	# of Claims	OWNER	EXPIRY_DATE
YD97107	Quartz	Active	WOLF 147	1	White Gold Corp. - 100%	2025-02-15
YD97108	Quartz	Active	WOLF 148	1	White Gold Corp. - 100%	2024-02-15
YD97109	Quartz	Active	WOLF 149	1	White Gold Corp. - 100%	2025-02-15
YD97110	Quartz	Active	WOLF 150	1	White Gold Corp. - 100%	2024-02-15
YD97111	Quartz	Active	WOLF 151	1	White Gold Corp. - 100%	2025-02-15
YD97112	Quartz	Active	WOLF 152	1	White Gold Corp. - 100%	2024-02-15
YD97113	Quartz	Active	WOLF 153	1	White Gold Corp. - 100%	2025-02-15
YD97114	Quartz	Active	WOLF 154	1	White Gold Corp. - 100%	2024-02-15
YD97115	Quartz	Active	WOLF 155	1	White Gold Corp. - 100%	2025-02-15
YD97116-YD97190	Quartz	Active	WOLF 156-WOLF 230	75	White Gold Corp. - 100%	2024-02-15

Access and Infrastructure

There is no road access to the Wolf property. Currently the claims are accessible via helicopter from Dawson city, located 120km north-east, or the community of Beaver Creek, located approximately 80km southwest. The property is also accessible by small, fixed wing airplanes to the Thistle Airstrip (E6995390, N586256 NAD 83, Zone 7N) followed by a 35km helicopter flight from White Gold's Thistle Camp (Figure 1).

For the 2023 program, White Gold's Thistle camp supported the exploration activities. Crews were provided accommodations at the Thistle Camp and transported daily to and from the project area via helicopter.

Physiography

The Wolf claims encompass an area of fully to partially vegetated hills within the Dawson Range mountains, incised by a combination of mature dendritic drainages and more steep mountain faces. Elevations range from 400masl at the White River to 1,560masl at Wolf Mountain.

At lower elevations vegetation is a typical boreal forest consisting of white spruce, birch and poplar on well-drained slopes and black spruce on poorly drained, and often permafrost covered north facing slopes. North facing slopes are underlain by permafrost and are sparsely populated by stunted black spruce. As topography increases, vegetation transitions from tree to moss and low bush cover. In regions of steeper topography ground cover is typified by talus, felsenmeer, and varying concentrations of moss. Typical of the Dawson Range, the Wolf property was not previously glaciated. A photograph of the typical physiography of the Wolf property is shown in Photo 1.

Climate

The region has a subarctic continental climate, with a mean temperature of -4.4° C. The temperature reaches over 30° C in the summer and can drop below -50° C in the winter. Summer daylight hours peak at 19 hours, 8 minutes of daylight in June, dwindling to a minimum of 5 hours, 38 minutes in December.



Photo 1. Typical Physiography of the Wolf Property

2.0 GEOLOGY

2.1 Regional Geology

The Wolf property is located within the Yukon-Tanana (YT) terrane of western Yukon and central Alaska. The YT is an accreted terrane of polymetamorphosed and polydeformed metasedimentary, metavolcanic, and metaplutonic rocks of Upper Paleozoic and older ages bounded by the Tintina Fault to the northeast and Denali Fault to the southwest (Figure 3). Overall, it records a prolonged and complex history of tectonic and magmatic processes along the northwestern margin of Laurentia between the Middle Paleozoic and Early Tertiary. It has an equally complex metallogenic evolution with at least 10 pulses of mineralization of various styles currently recognized (Nelson et al., 2013, Allan et al., 2013, Mortensen and Allan, 2012).

In the area of the Wolf property, bedrock consists of metasedimentary and metavolcanic rocks of the Devonian-Mississippian Nasina Assemblage and Simpson Range Suite that are cross-cut/overlain by the Permian Snowcap and Klondike assemblages. These units underwent ductile (D1/D2) deformation associated with amphibolite facies metamorphism during the Late Permian Klondike Orogeny. This event was associated with the accretion of the YT terrane to Laurentia and associated closure of the Slide Mountain Ocean and obduction of ophiolitic slices of the Slide Mountain terrane.

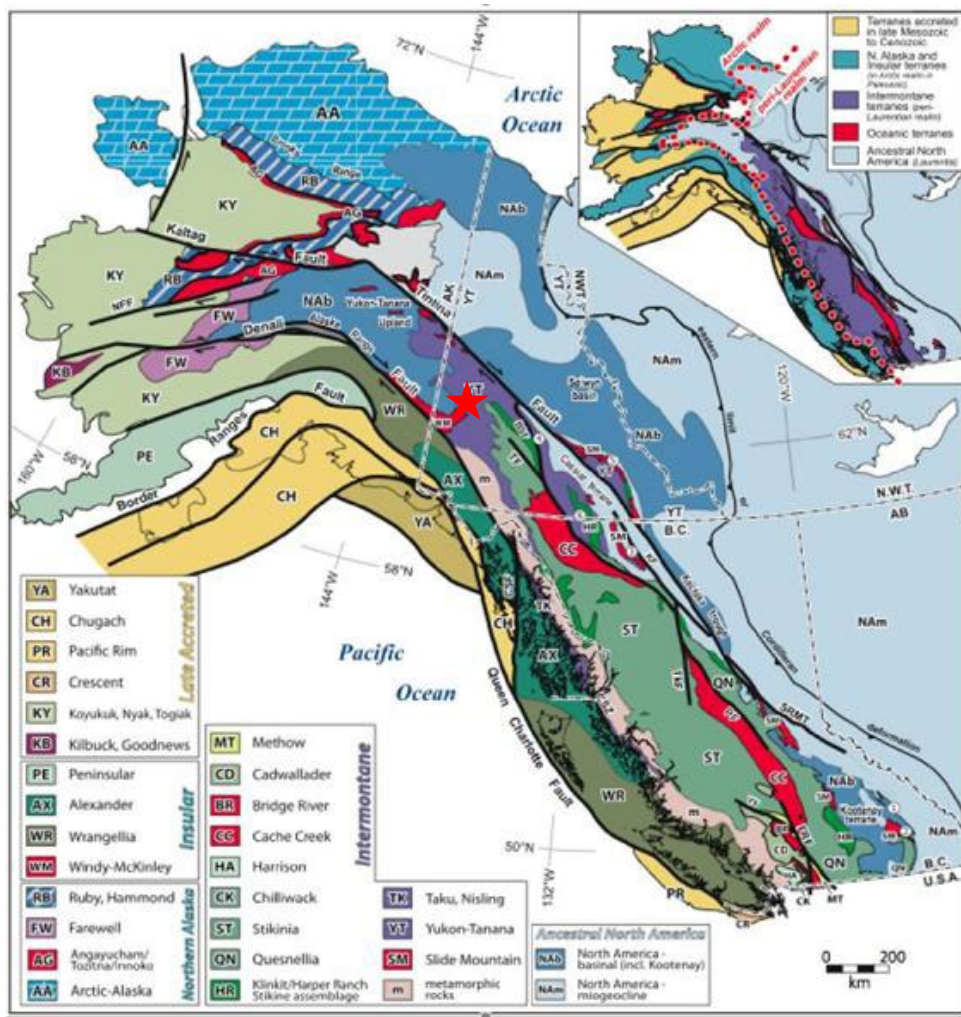


Figure 3. Terrane map of the northern Cordillera (modified from Nelson et al 2013). The red star is the approximate location of the property.

The area underwent additional compression and ductile deformation (D3) associated with greenschist facies metamorphism during the Late Triassic-Early Jurassic. The event was associated with widespread thrust faulting and imbrication of the Slide Mountain terrane, and the emplacement of felsic to ultramafic intrusions. This transitioned into a period of regional uplift and exhumation and is associated with dominantly east-west oriented sinistral faults, localized north-northwest vergent folds, and high angle reverse faults (D4). This period of deformation spans the ductile to brittle transition and are associated, particularly the E-W sinistral faults, with 'orogenic' style gold mineralization throughout the White Gold and Klondike districts.

Renewed northeast dipping subduction under the continental margin during the Late Cretaceous led to renewed magmatism across the YT terrane and is associated with felsic to intermediate intrusions of the Dawson Range Batholith and felsic-mafic volcanic rocks of the Mount Nansen Suite. The Early Cretaceous arc activity ceased around 99Ma, at which point it stepped farther inboard and is associated with intrusive suites in the Selwyn Basin (i.e. Tombstone Suite, etc.). This lull in magmatism was associated with deposition of the Indian River Formation, a coarse clastic sedimentary package deposited in an alluvial/fluvial to shallow marine setting that records approximately 40 million years of sedimentation following the formation of the Dawson Range Arc.

Arc style magmatic and volcanic activity renewed during the Late Cretaceous and is associated with a series of calc-alkaline plutons and high-level porphyry dikes, plugs, and breccias in the Casino, Freegold,

and Ford areas, and age equivalent intrusions in eastern Alaska (79 – 72Ma). This event was also likely associated with the initiation of dextral offset along the Big Creek Fault and reactivation of older Jurassic age structures in Dawson Range area. It is also associated with variable styles of mineralization ranging from Cu-Au-Mo porphyries (Casino), intrusion-related/epithermal occurrences (Sonora Gulch, Freegold area), and structurally controlled gold / 'orogenic' mineralization (Coffee, Boulevard, Moosehorn). At 72Ma there was a distinct change in magmatism with widespread bi-modal volcanism (Carmacks Group) and the emplacement of small, high-level, felsic plugs and stocks (Prospector Mountain Suite) throughout the YT terrane. A prominent set of northeast trending normal and sinistrally oblique faults are commonly associated with the intrusive and volcanic rocks of this event and are broadly coeval with magmatism.

A final magmatic event occurred during the Late Tertiary and is associated with the emplacement of bi-modal suite of predominately north-south trending dike swarms, plugs, and local pyroclastic rocks. Gabrielse et al. (2006) suggests that the magmatic event was likely coeval with the early stages of dextral offset along the Tintina Fault.

2.2 Property Geology

The broader geology of the Wolf property was best summarized by Tallman (2012) as part of Ethos Gold Corp.'s ("Ethos") 2011 work on the property. Mr. Tallman's property geology description is provided below:

"Rocks within the Wolf property area consist of Jurassic-age granodiorite, probably a phase of the Aishihik Suite, which intrude the Devonian and Mississippian-aged quartz-mica schist to paragneiss Nasina Assemblage (410-323 Ma, DMN₃). A body of possible Permian-aged K-feldspar augen-bearing orthogneiss lies 1 km-northeast of the property (Pautler, 2011). A small intrusive body of medium-grained, weakly porphyritic hornblende-biotite granite was delineated at the Aries showing with local, pink-weathering K-feldspar alteration (Jilson and Brownlee, 2000). Andesite and basalt flows, locally with plagioclase phenocrysts, of the Upper Cretaceous Carmacks Group (uKC) underlie the northeastern Wolf and Cu claims and cover the older lithologies (Pautler, 2011) (Figure 4). At the base of the Carmacks Group, thin layers of fragmentals and rhyolite tuff with up to 10% pyrite have been observed. Jilson and Brownlee (2000) suggest that the contact between the Klondike Schist and the Carmacks Group volcanic rocks is a fault with the Carmacks side down-dropped.

Numerous north-northwesterly trending fault structures have been inferred in the claim area; a northeast trending fault was also observed near the Aries showing. Based on topographical/aerial and aeromagnetic lineaments, the Big Creek fault (which extends through the Freegold and Sonora Gulch properties) may extend northwesterly along the Yukon River then along a major lineament northeast of the property (Pautler, 2011). The possible northwestern continuation of the Coffee Creek structure (identified by an aeromagnetic low), which is known to extend through the Latte zone on the Coffee Property, may actually be the Big Creek Fault (Pautler, 2011). A lineament located approximately 5 km northeast of the property may be the continuation of this structure. "Newmont Corporation's Coffee project, situated 40 km southeast of Wolf, has documented significant gold mineralization along the Coffee Creek structure" (Tallman, 2012).

Subsequent to Ethos, mapping conducted by consulting structural geologist Dr. Michael Cooley in 2017, furthered the local geological understanding of the property by conducting detailed mapping of a variety of lithologies, alteration, and mineralization styles. A summary of Cooley's mapping and local geology is provided below (Cooley, 2017), and a local geology map modified from Cooley's 2017 mapping is provided in Figure 4.

Lithologies

Metamorphic Basement Rocks

In the Wolf target area, the oldest rocks are comprised of isolated and infrequent patches of metasedimentary float boulders, which are primarily composed of micaceous schist and gneiss. These patches of metamorphic rocks have undergone significant biotite and/or potassic alteration and are interpreted to represent minor rafts or roof pendants that occur within a widespread hornblende biotite diorite intrusion.

Hornblende Biotite Diorite

A generally massive, non-foliated medium to coarse grained intrusive consisting of hornblende, biotite and plagioclase underlies most of the Wolf target area. Although mainly diorite in composition, texturally identical rocks locally contain minor K-feldspar and / or quartz, suggesting this intrusion varies compositionally between monzonite and quartz diorite. Alteration in this unit varies from mainly unaltered to weakly biotite altered, with igneous hornblende slightly to completely altered to shreddy texture hydrothermal biotite throughout the mapped areas of this pluton. Local zones of strongly biotite altered occur locally.

Fine Grained Acicular Hornblende felsic intrusive

Although this unit was too small to distinguish on the geologic map, a small scree slope of felsic, fine-grained dikes containing a feldspar matrix with 1% coarse, blocky feldspars, and 2% fine-grained, acicular hornblende can be found northeast of the main gold soil anomaly in the southwest grid area. In one outcrop example, a 50 cm-wide dike is seen cross-cutting hornblende diorite.

Carmacks Volcanics

The Carmacks volcanics consists of an upper level of andesitic flows, amygdaloidal flows and lapilli tuffaceous rocks underlain by a clast-dominated lithology that consists of heterolithic clast conglomerate. Clasts of diorite are commonly found within the conglomerate, which implies that the Carmacks sits on top of an erosional surface underlain by the diorite. Although mapped as felsic volcanics on the government compilation map, it's hypothesized that the pervasive biotite alteration and/or potassic alteration has made this unit only appear felsic and the protolith is mafic to intermediate.

Granite

A medium to coarse grained granite occurs mainly in the northern part of the Wolf map area which is assumed to be the earlier phase. This unit is generally pink to light orange. A megacrystic Kspar granite, which has the same colour and mineral composition as the medium grained unit is assumed to be younger and more coarse grained phase of essentially the same granite source. Abrupt changes in soil geochemistry and the interpreted map pattern for the granite implies that the granite cuts mineralization and the Carmacks Volcanics, and may be a possible source for fluids for the widespread biotite and potassic alteration. The granite itself locally shows weak biotite alteration in the form of shreddy biotite replacement of some hornblende phenocrysts. The surface extent of this unit shown in Figure 4 has been largely interpreted by using the radiometric aero-geophysical data.

Alteration

Potassic

A few central cores of strong potassic alteration have been recognized in the southwestern soil grid area at Wolf. One area of strong potassic alteration coincides with anomalously high gold and copper in soils in the southwest soil grid area, which has been named the Taurus target.

Strong Biotite

Commonly with the potassic alteration is abundant hydrothermal biotite that occurs with shreddy textures replacing mafic minerals, and as a disseminated fine grained biotite throughout the rock. Textures of this strong biotite alteration can be described as “sooty” where they consist of pervasive fine grained biotite occurring throughout the rock matrix and along fractures as biotite veinlets. Strong biotite alteration forms an envelope that surrounds the apparent high temperature potassic altered cores.

Weak Biotite

Peripheral to the strong biotite alteration is a wide zone of discontinuous weak biotite alteration identified by selective replacement of hornblende crystals by shreddy texture biotite.

Magnetite

Within the potassic and strong biotite zones there is common but generally weak evidence for magnetite alteration in the form of thin magnetic veinlets or weakly magnetic shreddy biotite patches after hornblende. Where mapped to date, the alteration at Wolf evidently does not include zones of intense magnetite replacement.

Structures

In the southwest soil grid area (Taurus target), there may be a structure or structures within the zone of copper and gold mineralization that likely strike sub-parallel to the adjacent granite dike (Figure 4). The granite dike may locally intrude parallel to the mineralized zone, or along a parallel splay. Additional prospecting may be advised within the cores of the zones of high gold to better understand the nature of these soil anomalies.

Mineralization

The copper anomaly at the Aries showing occurs mainly within Carmacks andesite and basaltic flows where it lies in contact with adjacent megacrystic Kspar granite to the north (Figure 4). The copper could be a contact metamorphic effect where the mafic volcanics are in contact with the granite. The main gold in soil anomaly (the Taurus target) in the southwestern soil grid at Wolf occurs mainly within diorite and is interpreted to occur along a structure that is sub-parallel to the adjacent granite dike to the north. The granite dike may be a dilatant zone along a major east-west shear zone as interpreted from the Yukon regional aeromagnetic anomaly map.

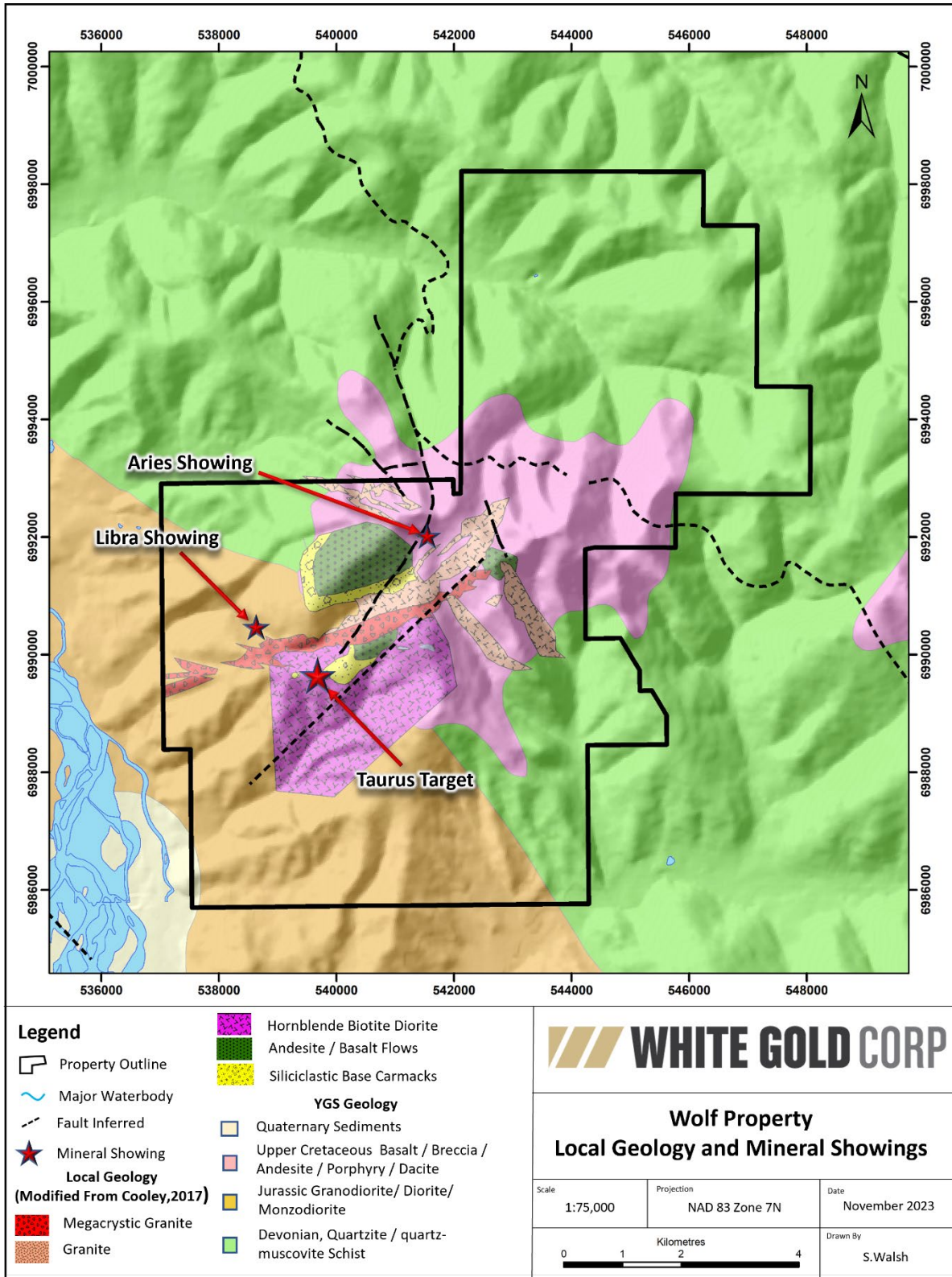


Figure 4. Local Geology of the Wolf Property with Mineral Showings. Modified from Cooley, 2017 and YGS.

3.0 PREVIOUS EXPLORATION WORK

A summary of all recorded historical mineral exploration on the Wolf property is provided below, along with significant results from each exploration campaign. A compilation figure (Figure 5 and Figure 6) illustrating significant historical geochemical survey results is provided at the end of the section.

1970: Quintana Minerals

The first recorded exploration on the present-day Wolf property occurred in the north-eastern region of the property in 1970 when Quintana Minerals (“Quintana”) prospected the region looking for copper porphyry targets similar to the Casino deposit. No assessment report was filed from their work, however, after staking the property, Quintana proceeded to conduct a field program of grid soil sampling, geological mapping, and bulldozer trenching. Results from this program appear to have uncovered magnetite, pyrite, pyrrhotite, chalcopyrite, and molybdenum mineralization along the Carmacks Group volcanics-intrusive contact. This mineral occurrence became known as the Aries showing. No additional work is recorded by Quintana following their 1970 field season. A photograph of the Aries showing is provided below in Photo 2. The historical trenches have since been naturally re-vegetated by alder and spruce trees.



Photo 2. Aries Showing. Historical Bulldozer trenches re-vegetated by trees.

1971: Astor Mines and Marguerite Lake Mines (JV)

In early 1970, an area in the southwestern region of the present-day Wolf property was staked by Al Carlos, who subsequently optioned the claims to Astor Mines Ltd (“Astor Mines”). An airborne magnetic survey was completed in 1971 after optioning the property to a joint venture between Astor Mines and Marguerite Lake Mines. The survey was centered overtop of the Libra showing, however, no specific geological or mineralogical information regarding this showing was recorded. Anecdotal accounts suggest the Libra showing represents a strong magnetic high, identified in the airborne survey (Watson, 1971).

1994: O. Davis

In 1994 prospector O. Davis re-staked the Aries showing. No records of subsequent exploration work were submitted by Mr. Davis to the mining recorder and the claims subsequently lapsed.

1998: Shawn Ryan

In 1998 the Aries showing was staked by local prospector Shawn Ryan with the goal of identifying a buried porphyry deposit which he felt could be present based on the historic soil geochemistry (Ryan, 1998). Mr. Ryan and a field assistant spent a total of 6 days resampling and characterizing the trenches excavated by Quintana in 1970. Results from the 1998 exploration program by Mr. Ryan identified a gold-copper geochemical correlation from samples collected around the old Aries trenches. In addition to locating disseminated molybdenum mineralization within 1-2-inch-wide quartz veins a volcanic breccia with anomalous silver, lead, antimony, and bismuth was located within the historical trenching area suggestive of porphyry style mineralization (Ryan, 1998).

1999: Deltango Gold

In 1999 Deltango Gold Ltd (“Deltango”) staked to the west and east of the Aries showing (held at the time by Mr. Ryan) and commenced a field program which involved the collection of 43 silt samples, 68 pan concentrate stream samples, 37 soil samples, and 26 rock samples. Deltango’s field program identified a porphyry unit (unit 5) which they deemed to be suggestive of a copper-molybdenum porphyry system with peripheral base and precious metal veining (Jilson and Brownlee, 2000). No further work was reported by Deltango on these claims.

2005: Shawn Ryan

In 2005 Shawn Ryan returned to the Aries showing and conducted a small prospecting program in the vicinity of Quintana’s 1970 trenches.

2008: Shawn Ryan

Mr. Ryan returned to the property in 2008 and collected ridge and spur soil samples around the Aries showing (Ryan, 2008). Results from the soil sampling program identified a relatively contiguous gold-antimony-copper- and molybdenum anomaly which appears to be associated with an intrusive unit, and continued to support his theory that a buried porphyry could be present at the Aries target (Ryan, 2008).

2009: Shawn Ryan

In 2009 Shawn Ryan staked an additional 42 claims to the southwest of his existing claim package, to form a larger contiguous property. Overtop of these claims, Mr. Ryan and a team of prospectors collected 542 soil samples and conducted 16 line km of ground magnetic surveying. The 2009 soil sampling program was designed to follow up on prospective soil samples collected in 2008. Results of the soil sampling program identified three parallel, NE-SW oriented gold in soil anomalies which remained open in both directions. Results from the ground magnetic survey which was conducted overtop of the soil sampling grid also identified a primary NE-SW trend, subparallel to the gold in soil anomaly (Ryan, 2010).

2010: Shawn Ryan

In 2010 Shawn Ryan returned to the property and staked an additional 188 claims (Wolf 43-110, Wolf 111-230), to the northwest and south of his existing claims. Following this staking, Mr. Ryan optioned the property to Ethos Gold Corp (“Ethos”) in late 2010.

2011 Ethos

After optioning the property from Shawn Ryan, Ethos commenced a field season which involved the collection of 2,194 soil samples, prospecting, rock sampling, airborne magnetics and radiometric surveying, air-photo imaging, and the completion of a technical report (Tallman, 2012). The objective of Ethos’s field program was to identify a bulk-tonnage gold deposit with the potential to host 3M oz of gold.

Results from the soil sampling program identified a continuous 5km x 1.5km northeast-southwest oriented gold in soil anomaly that remained open to the southwest. Gold in soil values in this anomaly ranged from 10-358 ppb Au.

Prospecting in 2011 focused on sampling the historic trenches created by Quintana in 1970. From this program, 18 rock samples were collected. None of the rocks collected from the trenches by Ethos were anomalous in gold or silver (Tallman, 2012).

A 553.2 line km airborne geophysics survey was flown by New-Sense Geophysics Limited (“New-Sense”), which at the time, covered the entire Wolf property. Survey results suggest the gold in soil anomaly identified at the property occurs along the contact of a northeast oriented radiometric high attributed to a granodiorite intrusion which cuts a quartz-mica schist (Tallman, 2012).

In 2011, Ethos also commissioned geologist Jean Pautler to write a technical report on the property (Pautler, 2011).

Due to a change in corporate focus, no further work was conducted by Ethos following their 2011 field program, however, additional work was recommended. Specifically, it was recommended to extend the soil grid to the southwest, and to prospect target areas where soil samples were unable to be collected due to the locally steep topography. A modest trenching program was also recommended overtop of the strongest portion of gold in soil anomaly (presently named the Taurus target) (Tallman, 2012).

2016: Shawn Ryan

In 2016, Shawn Ryan returned to the Wolf property and conducted an infill soil sampling program overtop of the Taurus target, the main gold in soil anomaly on the property. A total of 333 soil samples were collected from this program and added additional resolution to the main anomaly, returning gold in soil values up to 235 ppb Au (Fage et al., 2018).

2017-Present: White Gold Corp

2017

In 2017, White Gold Corp (“White Gold”) acquired the claims which comprise the Wolf property from Shawn Ryan. Since 2017 White Gold has remained the owner of the property.

In 2017, GroundTruth Exploration, on behalf of White Gold, conducted a multi-survey program on the property which involved the collection of 161 soil samples, mapping, prospecting, 227 GT Probe samples, 4.98 line km of resistivity and induced polarization (“RES/IP”) surveying over 12 lines, 75 km² of XCAM orthophotography, and 237.8 line km of airborne Dighem magnetics and electromagnetics (Fage et al, 2018).

The soil sampling program was focused on extending the main Wolf soil anomaly further to the southwest, while the GT Probe sampling, and RES/IP survey components of the program were all focused on better constraining the surface expression of the gold in soil anomaly.

Results from the soil sampling program did not extend the previously identified gold in soil anomaly any further to the southwest.

Results of the RES/IP survey overtop of the main gold in soil anomaly appear to show a sub-vertical dipping structure which is characterized by a Resistivity low.

The GT Probe program was successful in better constraining the bedrock source of the gold in soil anomaly, with one sample returning greater than 1 g/t Au (1.22 g/t Au). All GT probe rock samples which contained anomalous gold values also exhibited silicification and limonite alteration (Fage et al, 2018).

The mapping program was led by Dr. Michael Cooley and was successful in identifying and mapping numerous new units, and greatly increased the understanding of the local geology on the property. Lithological units identified during mapping include metamorphic basement rocks, hornblende biotite diorite, fine grained acicular hornblende felsic intrusive, Carmacks volcanics, and granite. When the local geology is superimposed against the gold in soil anomalies, it appears the copper anomalies appear to be associated with the Carmacks andesite and basaltic flows, whereas the gold in soil anomalies appear to be associated with mainly with the diorite, or siliciclastic basalt units (Cooley, 2017). The results of this mapping continues to form the basis of White Golds current understanding of the local property scale geology of the Wolf property.

2019

In 2019, GroundTruth Exploration, on behalf of White Gold conducted a modest exploration program comprised of prospecting, geological mapping, soil sampling, and GT Probe sampling which targeted the Taurus Target, the main gold in soil anomaly on the property. From this program, 10 prospecting rock samples, 666 soil samples, and 244 GT Probe samples were collected.

Soil sampling results from this program did not identify any additional contiguous gold-in-soil anomalies but did return locally high gold in soil values which reached up to 247 ppb Au.

Results from the GT Probe sampling returned modest gold values which reached up to 0.76 g/t Au (line WLFGTP19-002). The GT Probe program continued to define a NE-SW oriented gold bearing structure with sufficient resolution to merit future RAB drill testing (Banys and Crawford, 2019).

2022

In 2022, White Gold returned to the property to conduct a soil sampling, mapping/prosecting, and LIDAR topographic survey. From this program, a total of 268 soil samples, 20 rock samples, 10 mapping stations, and a property wide LIDAR survey was completed.

Soil sampling in 2022 focussed on extending the existing soil grid along the southwestern, southeastern, and northeastern aspects of Wolf Mountain. While the steep topography paired with the presence of scree along the southeastern slope of Wolf Mountain hindered the ability to collect soil samples in this area, soil samples were successfully collected along the other aspects. Mapping and prospecting also focused along the area of Wolf Mountain, along with the Aries showing.

The soil sampling program did not identify any additional significant gold in soil anomalies. The primary NE trending central gold in soil anomaly which hosts the Taurus target remains the primary drill ready stage exploration target.

Similarly, the mapping and prospecting did not return any material gold values outside of previously identified targets.

The property wide LIDAR survey was successful in generating property wide, high resolution topographic information which will be used for a detailed structural analysis of the property moving forward.

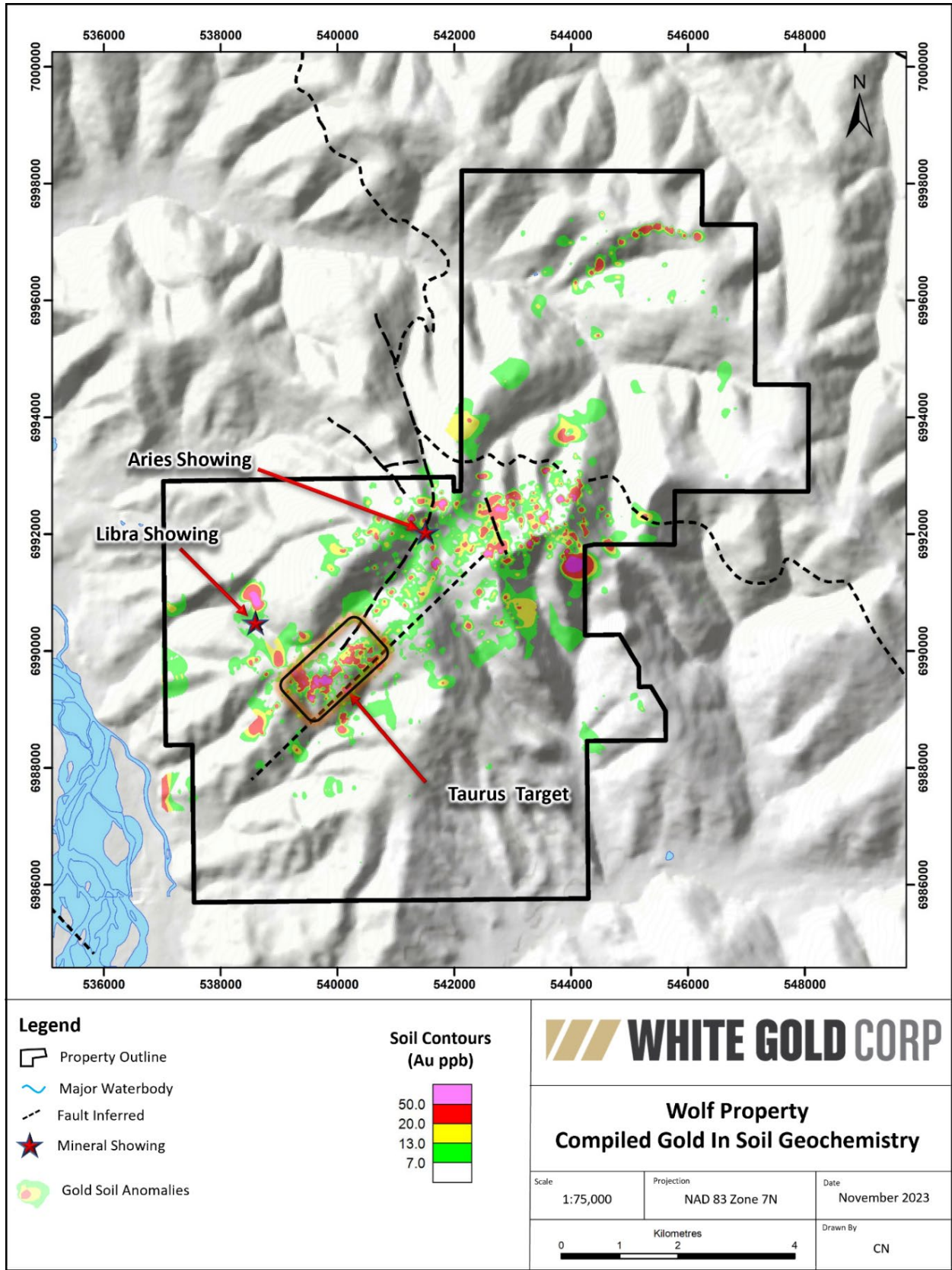


Figure 5. Compiled Gold in Soil Geochemistry of the Wolf Property

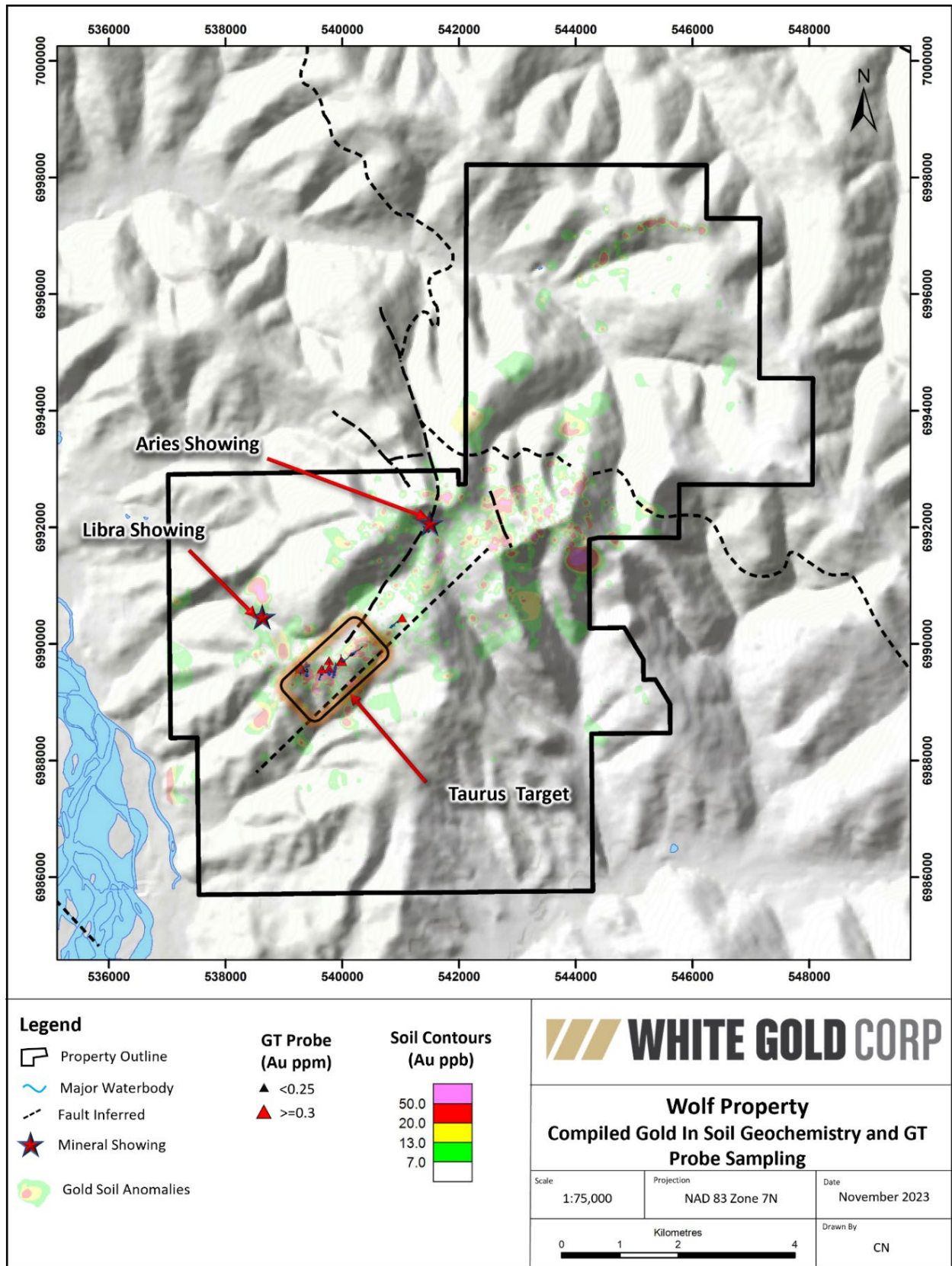


Figure 6. Compiled Gold in Soil Geochemistry and GT Probe Sampling

4.0 EXPLORATION TARGET

4.1 Targeted Mineralization

At present, gold mineralization at the Taurus target is the primary commodity of interest for White Gold. Geochemical analysis of the property suggests the Taurus target is a gold primary target, with gold only showing a weak correlation with silver, copper, arsenic, zinc, lead, bismuth, molybdenum, and antimony. A table showing the elements which show the strongest correlations with gold is provided below in Table 2

Table 2. Wolf Property Notable Gold Correlation Coefficients

	Ag	Cu	As	Zn	Pb	Bi	Mo	Sb
Au	0.25	0.24	0.35	0.31	0.13	0.25	0.25	0.15

Statistical percentile analysis from the compiled soil geochemistry supports the correlation coefficient table, with gold returning the strongest values. A table showing the percentile values of gold in soil geochemistry and other notable metals is provided below in Table 3.

Table 3. Wolf Property Soil Geochemistry Percentiles of Notable Metals

	Au	Ag	As	Zn	Pb	Cu
Population	1323	1323	1323	1323	1323	1323
Max Value	357.8	5.7	1293.4	1569	1000.9	365.1
Min Value	0.25	0.05	0.6	14	2.8	6.1
98th	66.344	0.8	114.044	128	54.512	69.424
95th	35.62	0.6	65.85	100	37.99	47.69
90th	19.9	0.5	39.28	86	28.28	38.86
85th	12.97	0.4	29.8	79	24.77	34.7
80th	9.76	0.3	23.56	73	21.5	32.5
70th	6.5	0.2	17.94	66	17.9	28.4
60th	4.9	0.2	14.6	61	15.4	25.7
50th	3.7	0.1	11.8	57	13	23.5
40th	2.9	0.1	9.8	54	10.8	21.8
30th	2	0.1	8.1	52	9.4	20

4.2 Deposit Model

Broadly, the exploration target model at the Wolf property's Taurus target is orogenic gold. The Wolf property is located within the regional, arcuate shaped Denali-Tintina fault zone which extends from the northern region of British Columbia through to Alaska. The province is underlain by rocks of the YTT and is characterized numerous gold deposits including: Pogo and Fort Knox, True North, Donlin Creek, Shotgun (Alaska), Golden Saddle (Yukon), and more closely Newmont's Coffee deposit (Yukon) (Tallman,2012).

At the target scale, analysis of the previously conducted IP survey at the Taurus target outlines a steeply dipping chargeability high underneath the gold in soil geochemical anomaly. Moreover, when the results of the compiled gold in soil geochemistry, GT Probe, lithology, and first vertical derivative magnetics are compared against one another (Figure 7), a relationship begins to emerge between these anomalies. When an outline of the gold in soil geochemistry anomaly at the Taurus target is overlaid onto the magnetics (first vertical derivative), the gold in soil anomaly appears to be associated with a magnetic low, with the same arcuate shape (Figure 7.B). Additionally, when the lithology as mapped by Cooley in 2017 is compared against the soil geochemical outline and GT Probe results, a relationship between the

Carmacks siliciclastic basement unit appears (Figure 7.C) to be a preferentially concentrated within siliciclastic basal units and/or andesite.

When the interpreted IP, GT probe, magnetics, and mapping data are interpreted in conjunction with one another, a deposit model emerges which suggests the Taurus target could be prospective for structurally hosted gold mineralization, with gold mineralization preferentially concentrated within the siliciclastic unit (Figure 9).

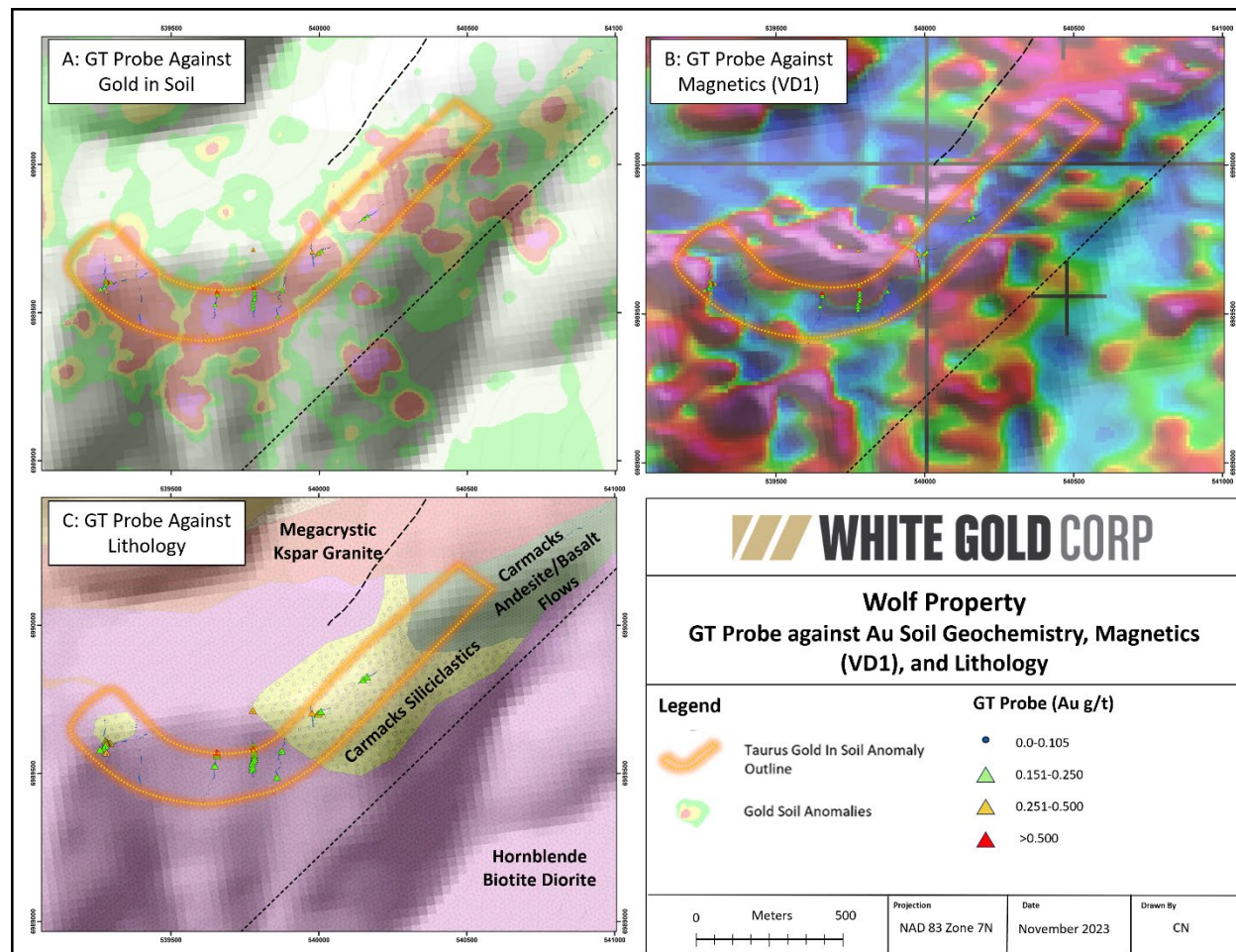


Figure 7. Relationships Between Gold in Soil, GT Probe, Magnetics, and Lithology of the Taurus Target

5.0 2023 EXPLORATION PROGRAM

Prior to 2023, no drilling campaigns had ever been conducted on the Wolf property. As part of the 2023 field season, an inaugural RAB drilling program was conducted on the Wolf property to test the Taurus target surface mineralization at depth. Four RAB holes, each planned to be 100m long, for a total of 400m of drilling were conducted to evaluate and enhance this prospect with the goal of advancing it to the diamond drill ready stage. A detailed description of the drilling program is provided below.

5.1 Rotary Air Blast Drilling

GroundTruth Exploration of Dawson, Yukon was contracted to provide drilling, downhole survey, and drill cutting interpretation for the 2023 Project. Remotely controlled, track mounted RAB drilling was

completed on the Taurus target between July 5th- July 11th, 2023. Four holes totalling 300.23m were completed as part of this program.

Drill moves between each drilling location were conducted by helicopter. While the RAB drill is track-mounted and can move under its own power, the use of the helicopter reduced the need for clearing vegetation between drill sites that the drill would otherwise have needed to traverse. Thereby, the environmental footprint of the program was reduced.

The specific purpose of the rotary air blast drilling was the following:

1. Targeting the strongest gold results identified in GT Probe (Figure 8) in the southwestern area of the Taurus target.
2. Test the apparent sharp sub-vertical contact between the magnetic low and high revealed by the 2017 IP survey line.
3. Target the gold anomaly outlined by GT Probe and soil sampling in the center of the Taurus target.
4. Undercut GT Probe line with anomalous gold mineralization in the eastern areas of the Taurus target.

The locations of the 2023 RAB drill holes are presented in figure 8, with the particulars of each hole presented in table 4.

Hole ID	Target	Easting (N83z7)	Northing (N83z7)	Elevation (m)	Azimuth (TN)	Dip	Length (m)
WLFTRS23RAB001	Taurus	540000	6989718	983	200	-50	86.87
WLFTRS23RAB002	Taurus	539294	6989624	932	200	-55	50.29
WLFTRS23RAB003	Taurus	539768	6989607	913	180	-55	92.96
WLFTRS23RAB004	Taurus	539777	6989515	898	000	-50	70.10

Table 4. Wolf 2023 RAB drill hole collar data

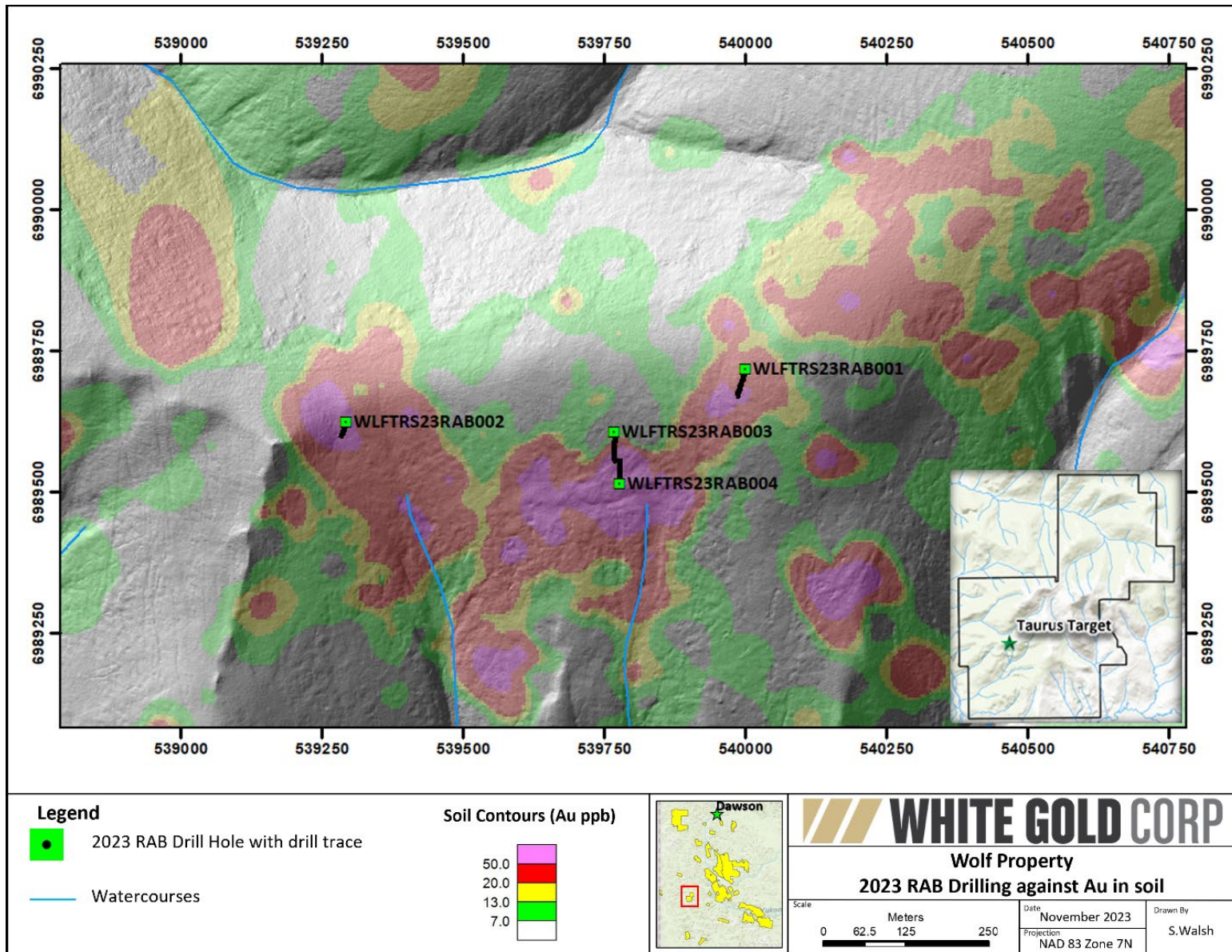


Figure 8. Location of Wolf RAB Drill Collars with drill traces against Au in the soil

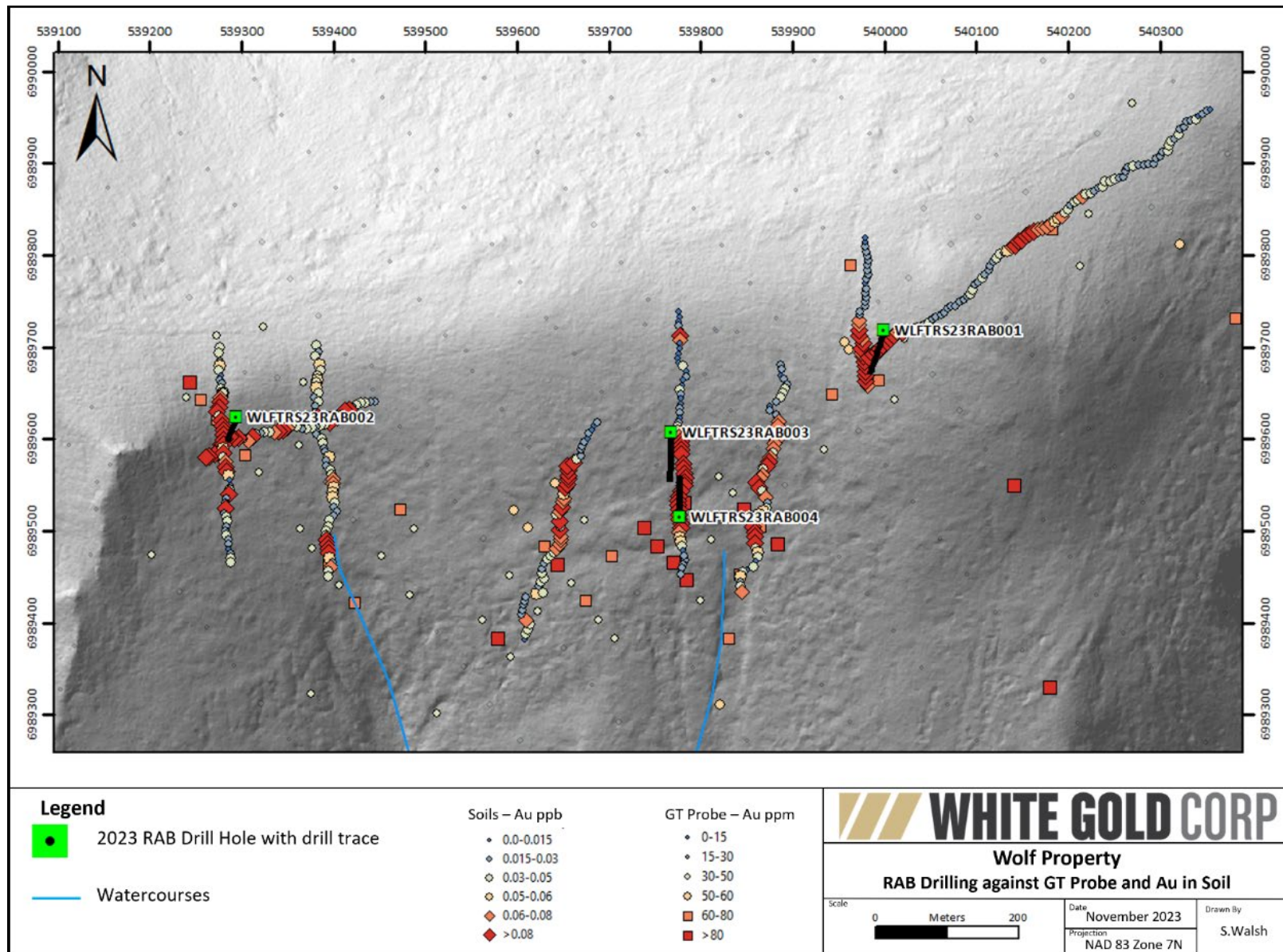


Figure 9. Wolf 2023 RAB Drilling Plotted Against GT Probe, gold in soil, and LiDAR

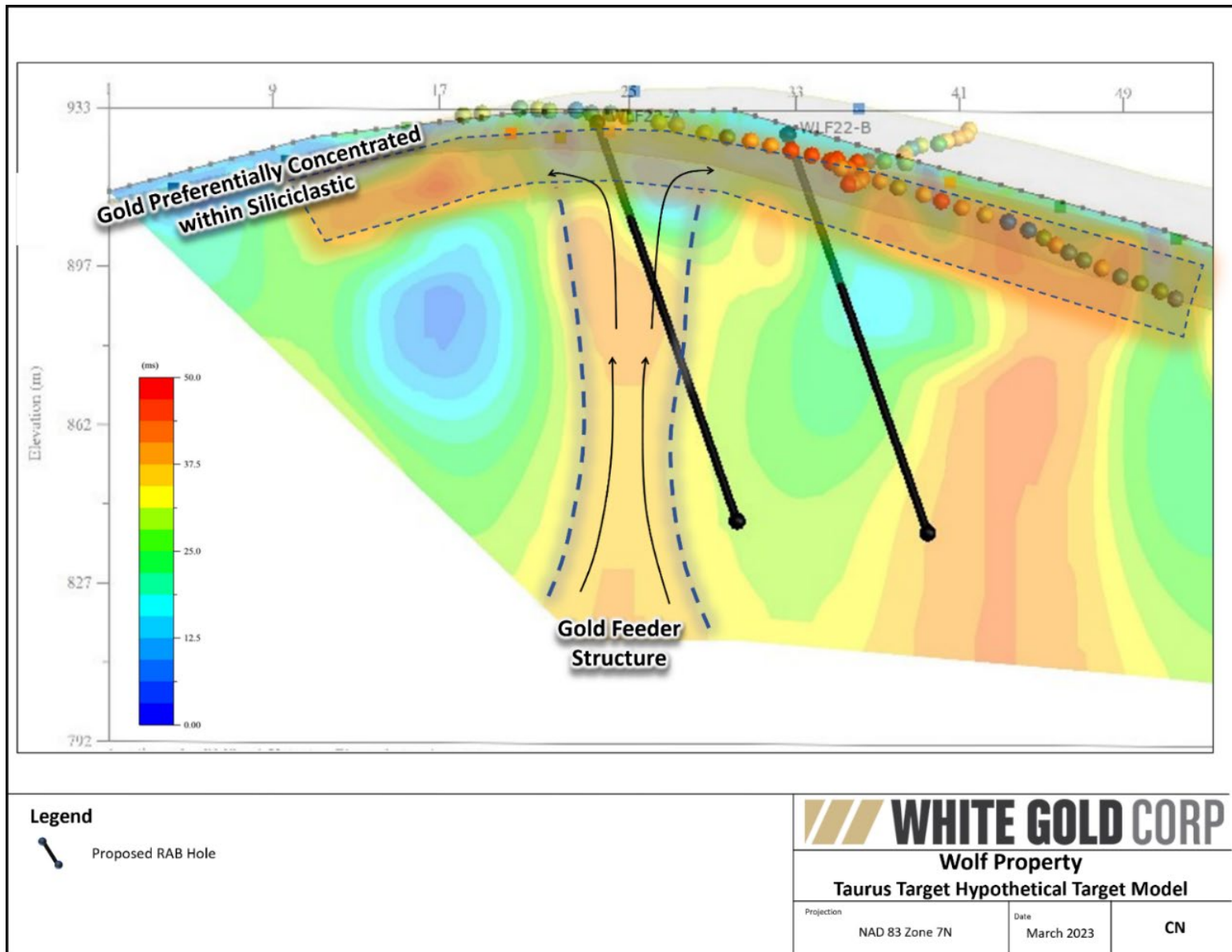


Figure 10. Conductivity Profile Across the Taurus Target Showing Proposed Target /Deposit Model and Planned RAB Holes

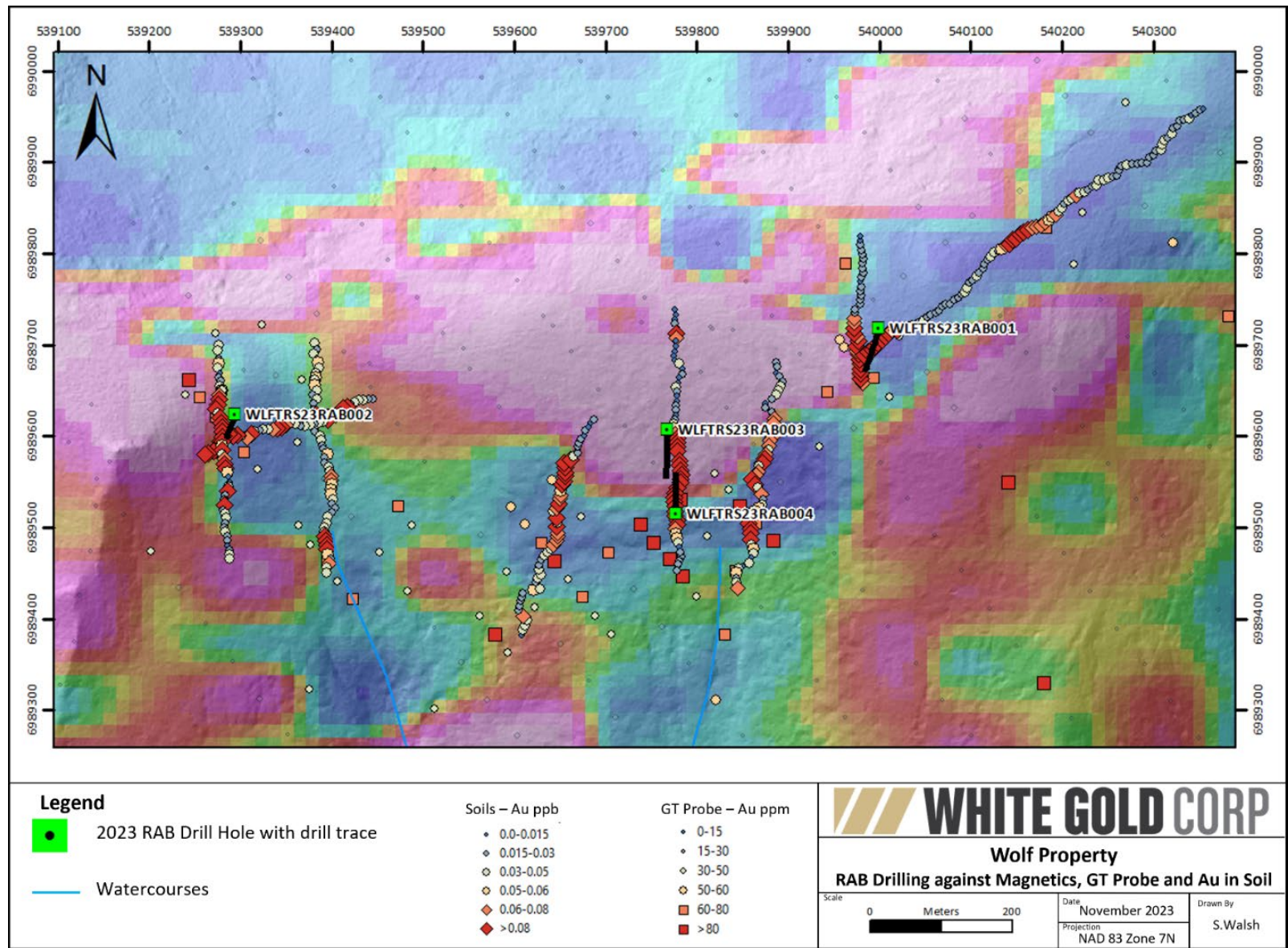


Figure 11. 2023 RAB Drilling Plotted Against First Derivative Magnetic, GT Probe, and Gold in Soil.

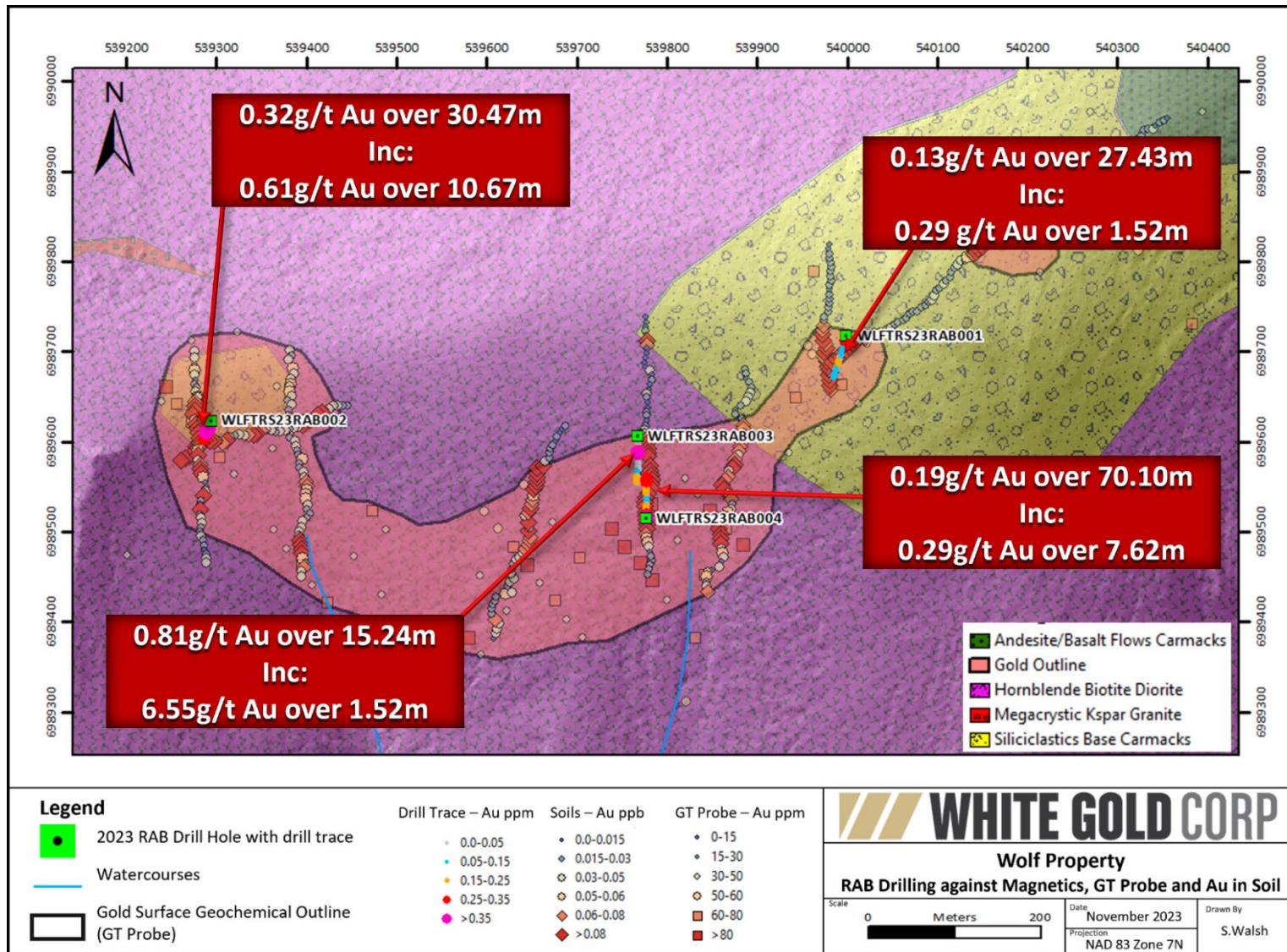


Figure 12. 2023 RAB Holes Plotted Against GT Probe (Au), Gold in Soil, and Lithology. Interpreted Surface Trace of Gold Anomaly and Gold assay values along RAB drill traces also shown

5.1.1 Procedures

Surveying

All 2023 drill hole collars were surveyed using a handheld GPS, the hole locations marked by a wooden picket denoting the hole number, azimuth, dip, and length. All holes drilled on the property were labelled with the prefix “WLF” followed by “TRS” (Taurus) “23” (the year) RAB00X (RAB hole number).

Drill sites which required ground leveling to support the RAB drill were recontoured as close as possible to their original slope. These sites continue to be monitored for revegetation. Due to the usage of a track-mounted RAB drill and site-to-site helicopter transport, vegetative mat disturbance was limited to 2 drill sites totalling 24m². If natural revegetation has not been established by the following season, additional revegetation and reclamation efforts will be undertaken.

A photograph of a typical RAB not requiring any ground manipulation is shown in Photo 3, and a typical RAB pad requiring ground manipulation is shown in Photo 4 below. In each photo, a labelled 4x4 wooden picket marking the hole location can be observed.



Photo 3. Typical RAB pad not requiring any ground manipulation or ground disturbance.



Photo 4. RAB pad requiring slight ground manipulation.

Downhole Surveys

Following the completion of each drill hole, a continuous downhole survey was completed using an optical televiewer. In addition to providing a continuous image of the borehole wall for use in geological interpretations, it provides a continuous drill trace orientation survey. This survey allows for detailed structural and geological analysis to be conducted and interpreted along side assay, XRF, and chip data.

Chip Delivery

Throughout the drilling process, representative chip samples were obtained, corresponding to the same 5ft intervals that assay samples were taken at. These samples were stored in chip trays and transported to Thistle Camp for storage and analysis. Chip trays were labelled at the drill site.

Chip Logging

Following the arrival of new chip trays at Thistle Camp, they were geologically logged by GroundTruth Exploration's onsite RAB geologist. Due to the nature of chip logging, descriptions were limited to lithology, with minor intervals of suspected mineralization highlighted. Additionally, handheld XRF analyses were taken of each sample interval. The raw data from these scans, along with the geological observations were recorded in a Microsoft Excel spreadsheet that was presented to White Gold as part of the contractor's deliverable as per their contract.

Chip Sampling

Sampling of RAB cuttings was conducted continuously along the length of the drill holes, with sample intervals of 5ft. The samples were collected at the drill site by GroundTruth personnel and placed in individual poly sample bags. After collecting the entirety of the sample, the sample tag corresponding to that sample interval was placed in the sample bag, and then the bag was sealed with a zip tie. Sealed sample bags were placed in pre-labelled rice bags, with each rice bag containing no greater than five samples. The rice bags were then sealed with both a zip tie and a security tag, before being stored in a secure location onsite to await transport to the laboratory.

Shipments were flown to Whitehorse or Dawson City for further ground transport by either a White Gold representative or a commercial trucking company to Bureau Veritas Mineral Laboratories (“BV Labs”) in Whitehorse, Yukon for analysis.

5.1.2 Sample Preparation

The 2023 RAB drill samples were prepared and analyzed by BV Labs. Once received at the lab, a confirmation code with an associated job number was emailed to White Gold by the preparation laboratory in Whitehorse. Once received and logged into BV’s tracking system, the samples were then dried, crushed, spit, and pulverized to 70% passing a 2mm screen. A 250g split was then taken and pulverized to greater than 85% material passing a 75-micron screen as per preparation code PRP70-250. Pulps were then sorted, labelled, and boxed prior to being shipped to BV’s analytical facility in South Vancouver.

5.1.3 Analytical Methodology

The prepared samples were analyzed for gold using the FA430 package (Au 30g fire assay fusion with AAS finish) and for 59 elements using MA-250 (4-acid digestion, ICP-ES/MS). For MA-250 analysis, a prepared sample (0.25g) is heated in HNO₃, HClO₄ and HF to fuming and taken to dryness. The residue is then dissolved in HCL. This process is referred to as “Ultratrace ICP-MS analysis” by BV Labs. If triggered, overlimit assaying was conducted for Ag, As, Cu, Zn, Pb, or Sb using assay package MA370. Table 5 presents the details of the applied analytical packages including their respective detection limits.

Code	Analytes and Ranges (ppm)							
FA430	Au	0.005-10						
MA-250	Ag	0.02-200	Eu	0.1-2,000	Nb	0.04-2,000	Ta	0.1-2,000
	Al	0.01%-20%	Fe	0.01%-60%	Nd	0.1-2,000	Tb	0.1-2,000
	As	0.2-10,000	Ga	0.02-100	Ni	0.1-10,000	Te	0.05-1,000
	Ba	1-10,000	Gd	0.1-2,000	P	0.001%-5%	Th	0.1-4,000
	Be	1-1,000	Hf	0.02-1,000	Pb	0.02-10,000	Ti	0.001%-10%
	Bi	0.04-4,000	Ho	0.1-2,000	Pr	0.1-2,000	Tl	0.05-10,000
	Ca	0.01%-40%	In	0.01-1,000	Rb	0.1-2,000	Tm	0.1-2,000
	Cd	0.02-4,000	K	0.01%-10%	Re	0.002-100	U	0.1-4,000
	Ce	0.02-2,000	La	0.1-2,000	S	0.04%-10%	V	2-10,000
	Co	0.2-4,000	Li	0.1-2,000	Sb	0.02-4,000	W	0.1-200
	Cr	1-10,000	Lu	0.1-2,000	Sc	0.1-200	Y	0.1-2,000
	Cs	0.1-2,000	Mg	0.01%-30%	Se	0.3-1,000	Yb	0.1-2,000
	Cu	0.1-10,000	Mn	1-10,000	Sm	0.1-2,000	Zn	0.2-10,000
	Dy	0.1-2,000	Mo	0.05-4,000	Sn	0.1-2,000	Zr	0.2-2,000
Er	0.1-2,000	Na	0.001%-5%	Sr	1-10,000			

Table 5. BV Labs Analytical Methods and Detection Limits for the 2023 Wolf RAB Drilling Program

5.1.4 QA/QC Program

A QA/QC program was completed for the 2023 RAB drilling program at the Wolf property which included the insertion of standards, blanks, and duplicates. Of the 207 samples submitted to the laboratory, 10 were QA/QC samples, representing an insertion rate of approximately 5%. Given that RAB samples are not commensurate for mineral resource estimation standards, this insertion rate is acceptable for the purpose of generally monitoring the performance of the laboratory. No QA/QC samples that were submitted returned assay values which fell outside of accepted values. It should be noted that for the duplicate samples which were submitted, none of the samples contained gold grades which allowed for material statistical analysis to be completed. A summary of the insertion rates for each QA/QC sample type is provided below in Table 6, and more detailed summary of the QA/QC submissions is provided in Table 7.

Type	Number of Samples	Insertion Rate
Chip samples	197	
Chip duplicates	3	1.5%
Standards	4	2.0%
Blanks	3	1.5%

Table 6. 2023 RAB Drilling QA/QC Sample Insertion Summary

QC Values				2023			
Standards	Accepted Value (Au g/t)	Lower Limit (Au g/t)	Upper Limit (Au g/t)	Number Submitted	Number Passed	Number Failed	Comments
CDN-GS-P5H	0.497	0.413	0.507	2	2	0	
CDN-ME-2106	1.641	1.362	1.920	1	1	0	
CDN-GS-7M	7.59	5.925	9.255	1	1	0	
BLANK			0.015	4	4	0	
DUPLICATE*		-30%	+30%	3	-	-	Assay values too low to be statistically material

Table 7. Summary of White Gold QA/QC Submissions for RAB Drilling Program

6.0 2023 EXPLORATION RESULTS

6.1 Rotary Air Blast

Detailed results of the 2023 RAB drilling program are presented below. Raw collected field data is provided in Appendix I, and BV certificates of analysis are provided in Appendix II.

In total, four RAB drill holes were completed on the Taurus target located within the Wolf property during the 2023 field season, producing a combined 300.23m of drilling. A summary of the drilling activities completed are provided in the subsections below.

6.1.1 Taurus Target

The 2023 RAB drilling at the Taurus target produced four drillholes totalling 300.22m, with hole lengths varying from 50.3m to 92.9m, with three holes oriented S or SSW (180°-200°) at dips ranging from -50° to -55, and one hole oriented N (360°) at a dip of -50° (see Table 4 above). Though no significant drill hole deviations occurred, hole caving and the interception of water caused a reduction in the length of all drill holes from their planned lengths.

A summary of each hole is provided below, with noteworthy assay intercepts from the Taurus target summarized in Table 7. Strip logs showing the gold grades intersected in each hole are provided in figure 9.

2023 Wolf Taurus Rotary Air Blast Drill Results				
Hole ID	From (m)	To (m)	Length (m)	Au (g/t)
WLFTRS23RAB001	0.00	27.43	27.43	0.13
<i>Inc.</i>	7.62	9.14	1.52	0.29
<i>Inc.</i>	18.29	19.81	1.52	0.11
	45.72	54.86	9.14	0.12

WLFTRS23RAB002	13.72	44.19	30.47	0.32
<i>Inc.</i>	18.29	28.96	10.67	0.61
<i>Inc.</i>	18.29	19.81	1.52	2.51

WLFTRS23RAB003	19.81	35.05	15.24	0.81
<i>Inc.</i>	21.34	22.86	1.52	6.55
	71.63	92.96	21.33	0.14
<i>Inc.</i>	77.72	80.77	3.05	0.18

WLFTRS23RAB004	0.00	70.10	70.10	0.19
<i>Inc.</i>	0.00	3.05	3.05	0.34
<i>Inc.</i>	62.48	70.10	7.62	0.29

Table 8. Wolf Taurus RAB Drilling Assay Summary

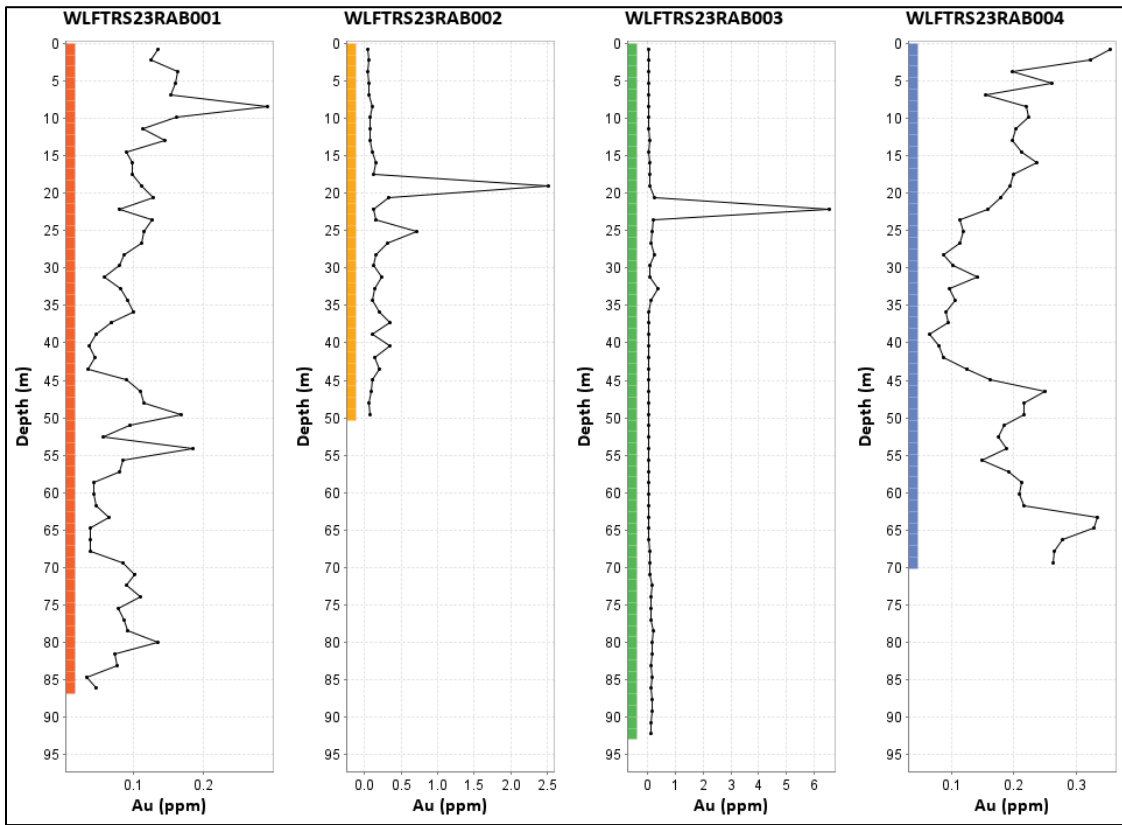


Figure 13. RAB drill downhole plot showing gold values vs. depth in meters. X-axis scale independent for each hole.

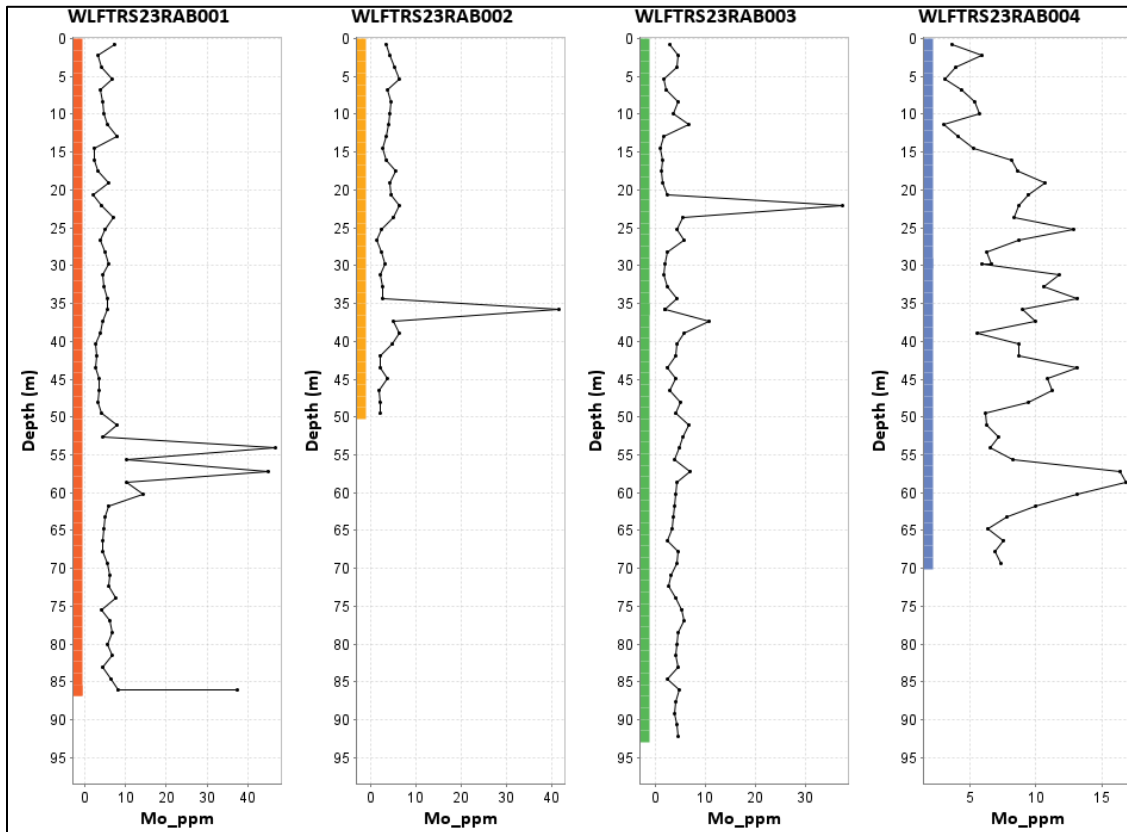


Figure 14. RAB drill downhole plot showing molybdenum values vs. depth in meters. X-axes independent for each hole.

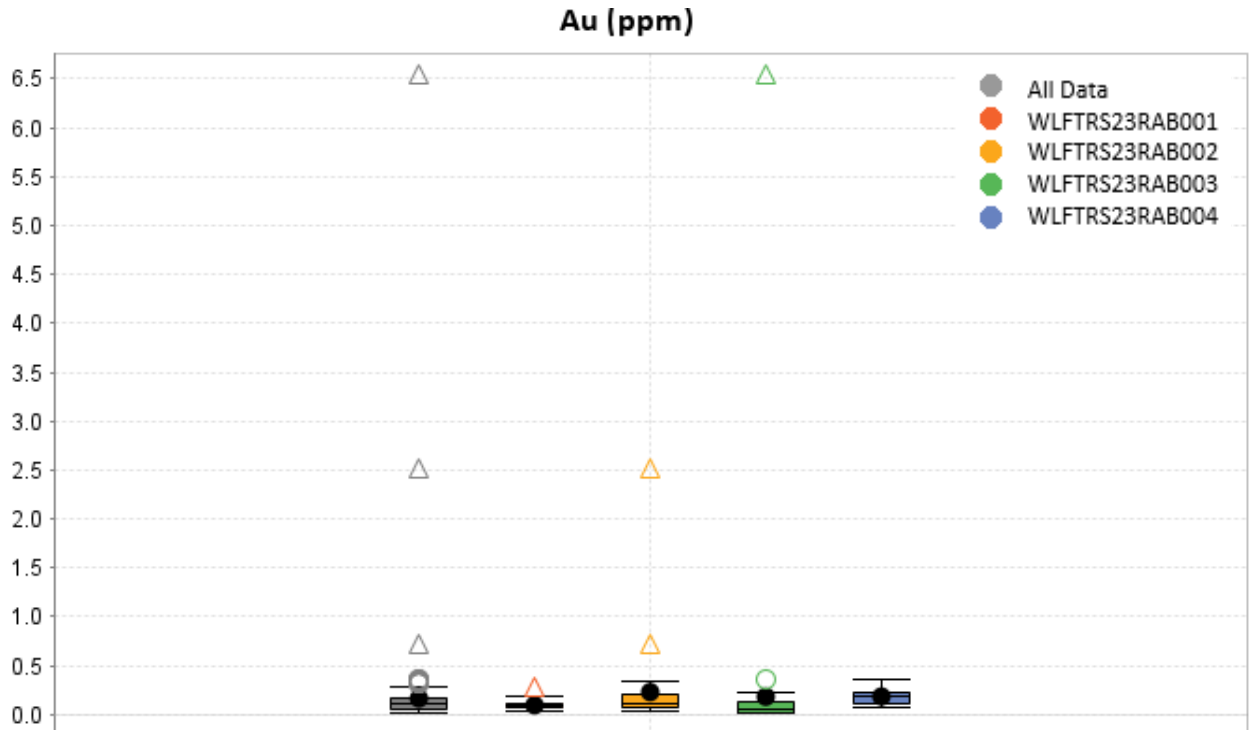


Figure 15. Tukey box and whisker plot showing gold assay results, including far outliers.

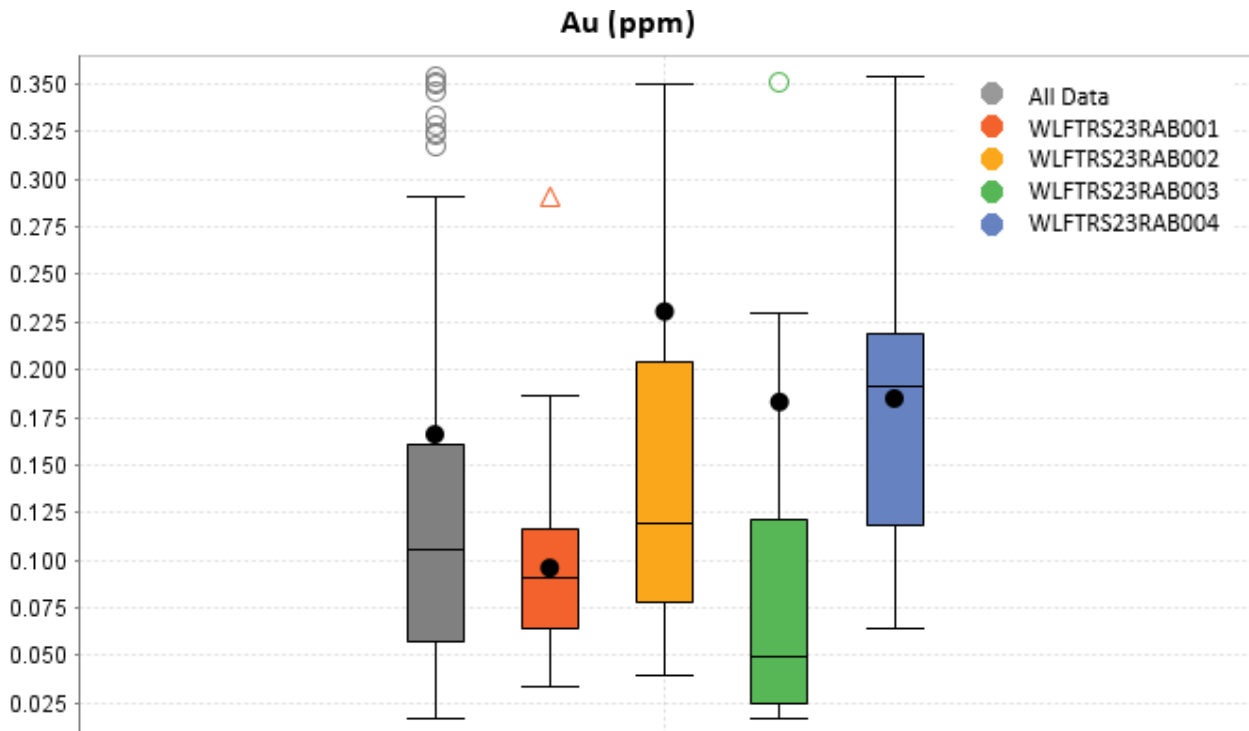


Figure 16. Tukey box and whisker plot showing gold assay results, excluding outliers.

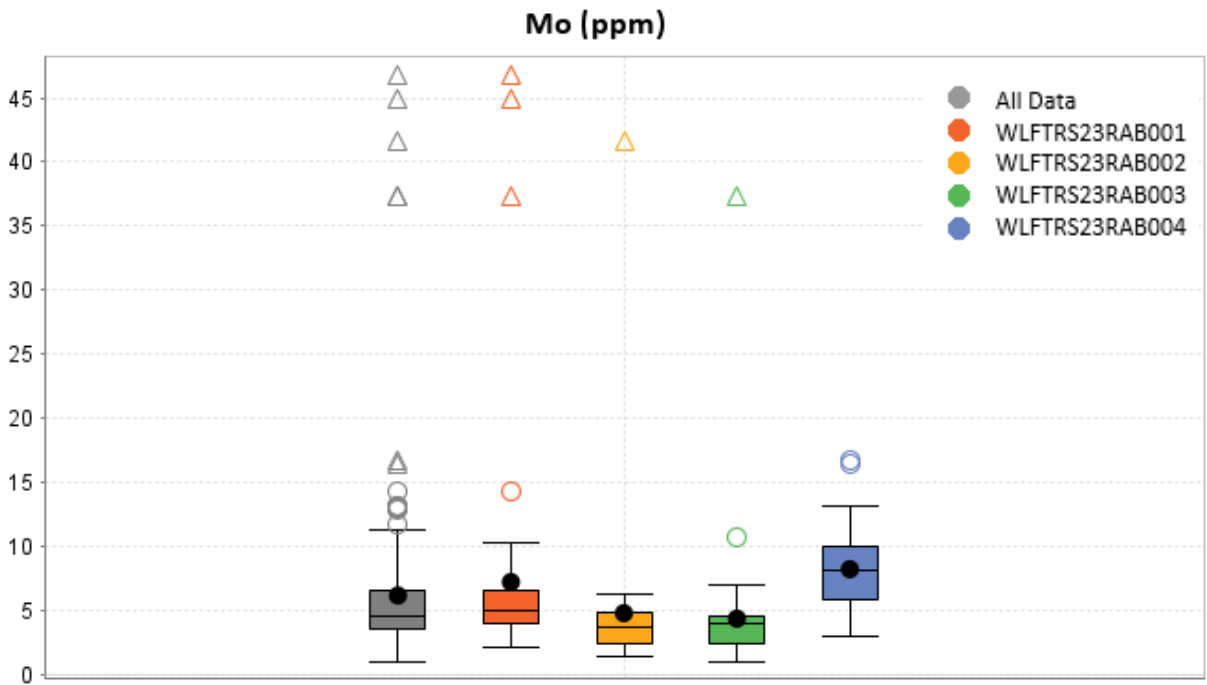


Figure 17. Tukey box and whisker plot showing molybdenum assay results, including outliers.

Based on the correlation matrix shown in Table 9 below, gold shows no strong nor consistent correlation with any major pathfinder elements or metals across the four 2023 RAB drill holes. Upon further investigation of the correlation tables in Table 10, a 0.924 gold/molybdenum correlation occurs in RAB003. Table 9 does show moderate to strong correlation (0.70-0.95) between Pb, Zn, Ag, as well as moderate correlation (0.45-0.70) between Co & Cu and Bi & As, possibly indicating a secondary phase of base metal enrichment. Table 10 exposes the strong variability in correlations in metals across the Taurus target area.

	Au ppm	Mo ppm	Cu ppm	Pb ppm	Zn ppm	Ag ppm	Ni ppm	Co ppm	As ppm	Sb ppm	Bi ppm
Au ppm	1.000	0.352	0.232	-0.003	0.027	0.092	0.186	0.057	0.097	0.209	0.004
Mo ppm	0.352	1.000	0.167	-0.036	-0.055	0.125	0.092	0.203	0.147	0.200	0.084
Cu ppm	0.232	0.167	1.000	-0.069	-0.052	0.236	0.383	0.541	0.325	0.109	-0.076
Pb ppm	-0.003	-0.036	-0.069	1.000	0.932	0.733	-0.073	0.031	0.087	0.411	0.115
Zn ppm	0.027	-0.055	-0.052	0.932	1.000	0.673	0.048	0.090	0.027	0.370	-0.008
Ag ppm	0.092	0.125	0.236	0.733	0.673	1.000	0.074	0.175	0.320	0.323	0.346
Ni ppm	0.186	0.092	0.383	-0.073	0.048	0.074	1.000	0.679	-0.084	-0.101	-0.303
Co ppm	0.057	0.203	0.541	0.031	0.090	0.175	0.679	1.000	0.091	-0.002	-0.108
As ppm	0.097	0.147	0.325	0.087	0.027	0.320	-0.084	0.091	1.000	0.266	0.489
Sb ppm	0.209	0.200	0.109	0.411	0.370	0.323	-0.101	-0.002	0.266	1.000	-0.034
Bi ppm	0.004	0.084	-0.076	0.115	-0.008	0.346	-0.303	-0.108	0.489	-0.034	1.000

Table 9. Correlation table of key elements from 2023 RAB drilling assay results

Logging of RAB chips, along with downhole optical televiewer imagery and systematic lithochemistry assays suggests a series of andesties, diorites, basalts, and small-scale quartz veining and breccias are the dominant lithologies drilled at the Taurus target. Periodic trace sulphides occurred throughout all lithologies to varying concentrations. RAB chip samples geologically logged by GTE staff as having light-moderate oxidation/alteration, grey-light grey-white andesite, and trace sulphides tended to contain the most enriched amounts of gold.

WLFTRS23RAB001											
	Au ppm	Mo ppm	Cu ppm	Pb ppm	Zn ppm	Ag ppm	Ni ppm	Co ppm	As ppm	Sb ppm	Bi ppm
Au ppm	1.000	0.088	0.297	0.045	0.020	0.117	-0.043	-0.018	0.263	0.212	-0.136
Mo ppm	0.088	1.000	0.208	-0.087	-0.063	0.287	0.462	0.427	0.227	0.217	0.086
Cu ppm	0.297	0.208	1.000	0.052	0.010	0.075	0.284	0.587	0.098	0.059	0.055
Pb ppm	0.045	-0.087	0.052	1.000	0.868	0.791	-0.017	-0.107	0.150	0.443	0.289
Zn ppm	0.020	-0.063	0.010	0.868	1.000	0.814	-0.004	-0.076	0.178	0.186	0.334
Ag ppm	0.117	0.287	0.075	0.791	0.814	1.000	0.240	0.134	0.375	0.382	0.369
Ni ppm	-0.043	0.462	0.284	-0.017	-0.004	0.240	1.000	0.727	0.000	-0.061	0.015
Co ppm	-0.018	0.427	0.587	-0.107	-0.076	0.134	0.727	1.000	0.017	-0.071	0.013
As ppm	0.263	0.227	0.098	0.150	0.178	0.375	0.000	0.017	1.000	0.454	0.281
Sb ppm	0.212	0.217	0.059	0.443	0.186	0.382	-0.061	-0.071	0.454	1.000	-0.006
Bi ppm	-0.136	0.086	0.055	0.289	0.334	0.369	0.015	0.013	0.281	-0.006	1.000

WLFTRS23RAB002											
	Au ppm	Mo ppm	Cu ppm	Pb ppm	Zn ppm	Ag ppm	Ni ppm	Co ppm	As ppm	Sb ppm	Bi ppm
Au ppm	1.000	-0.009	0.243	0.039	0.066	0.162	0.082	0.116	0.048	0.458	0.102
Mo ppm	-0.009	1.000	0.400	0.147	0.049	0.265	0.301	0.616	0.109	0.008	0.050
Cu ppm	0.243	0.400	1.000	0.024	-0.072	0.837	0.333	0.544	0.513	0.475	0.352
Pb ppm	0.039	0.147	0.024	1.000	0.287	-0.034	-0.114	-0.024	-0.005	0.218	-0.088
Zn ppm	0.066	0.049	-0.072	0.287	1.000	-0.286	0.571	0.378	-0.220	0.138	-0.320
Ag ppm	0.162	0.265	0.837	-0.034	-0.286	1.000	0.225	0.305	0.499	0.258	0.473
Ni ppm	0.082	0.301	0.333	-0.114	0.571	0.225	1.000	0.680	-0.170	0.017	-0.288
Co ppm	0.116	0.616	0.544	-0.024	0.378	0.305	0.680	1.000	0.094	0.086	0.062
As ppm	0.048	0.109	0.513	-0.005	-0.220	0.499	-0.170	0.094	1.000	0.279	0.665
Sb ppm	0.458	0.008	0.475	0.218	0.138	0.258	0.017	0.086	0.279	1.000	0.018
Bi ppm	0.102	0.050	0.352	-0.088	-0.320	0.473	-0.288	0.062	0.665	0.018	1.000

WLFTRS23RAB003											
	Au ppm	Mo ppm	Cu ppm	Pb ppm	Zn ppm	Ag ppm	Ni ppm	Co ppm	As ppm	Sb ppm	Bi ppm
Au ppm	1.000	0.924	0.457	0.002	0.034	0.108	0.638	0.145	0.518	0.241	0.035
Mo ppm	0.924	1.000	0.444	0.001	0.007	0.123	0.603	0.113	0.451	0.189	0.052
Cu ppm	0.457	0.444	1.000	0.303	0.363	0.409	0.622	0.514	0.603	0.282	0.314
Pb ppm	0.002	0.001	0.303	1.000	0.974	0.936	0.136	0.561	0.704	0.604	0.056
Zn ppm	0.034	0.007	0.363	0.974	1.000	0.937	0.199	0.603	0.767	0.605	0.134
Ag ppm	0.108	0.123	0.409	0.936	0.937	1.000	0.291	0.525	0.715	0.549	0.254
Ni ppm	0.638	0.603	0.622	0.136	0.199	0.291	1.000	0.300	0.501	0.254	0.327
Co ppm	0.145	0.113	0.514	0.561	0.603	0.525	0.300	1.000	0.756	0.717	0.021
As ppm	0.518	0.451	0.603	0.704	0.767	0.715	0.501	0.756	1.000	0.713	0.150
Sb ppm	0.241	0.189	0.282	0.604	0.605	0.549	0.254	0.717	0.713	1.000	0.015
Bi ppm	0.035	0.052	0.314	0.056	0.134	0.254	0.327	0.021	0.150	0.015	1.000

WLFTRS23RAB004											
	Au ppm	Mo ppm	Cu ppm	Pb ppm	Zn ppm	Ag ppm	Ni ppm	Co ppm	As ppm	Sb ppm	Bi ppm
Au ppm	1.000	-0.260	0.354	0.399	0.346	0.578	0.158	-0.152	-0.060	-0.186	0.323
Mo ppm	-0.260	1.000	0.303	-0.259	-0.093	-0.190	0.245	0.269	0.075	0.357	-0.311
Cu ppm	0.354	0.303	1.000	0.026	0.352	0.172	0.613	0.520	-0.388	0.023	-0.465
Pb ppm	0.399	-0.259	0.026	1.000	0.690	0.847	0.048	-0.075	0.202	-0.006	0.444
Zn ppm	0.346	-0.093	0.352	0.690	1.000	0.626	0.585	0.425	-0.122	0.038	-0.077
Ag ppm	0.578	-0.190	0.172	0.847	0.626	1.000	0.181	0.017	0.210	0.075	0.440
Ni ppm	0.158	0.245	0.613	0.048	0.585	0.181	1.000	0.917	-0.508	0.127	-0.616
Co ppm	-0.152	0.269	0.520	-0.075	0.425	0.017	0.917	1.000	-0.536	0.088	-0.703
As ppm	-0.060	0.075	-0.388	0.202	-0.122	0.210	-0.508	-0.536	1.000	0.659	0.520
Sb ppm	-0.186	0.357	0.023	-0.006	0.038	0.075	0.127	0.088	0.659	1.000	-0.142
Bi ppm	0.323	-0.311	-0.465	0.444	-0.077	0.440	-0.616	-0.703	0.520	-0.142	1.000

Table 10. Correlation tables for each 2023 RAB hole

6.1.2 RAB Hole Descriptions

- 0.0 - 1.52m**
- 1.52 - 3.05m**
- 3.05 - 4.57m**
- 4.57 - 6.10m**
- 6.10 - 7.62m**
- 7.62 - 9.14m**
- 9.14 - 10.67m**
- 10.67 - 12.19m**
- 12.19 - 13.72m**
- 13.72 - 15.24m**
- 15.24 - 16.76m**
- 16.76 - 18.29m**
- 18.29 - 19.81m**
- 19.81 - 21.34m**
- 21.34 - 22.86m**
- 22.86 - 24.38m**
- 24.38 - 25.91m**
- 25.91 - 27.43m**
- 27.43 - 28.96m**
- 28.96 - 30.48m**



WLFTRS23RAB001 tested the relationship between the Carmacks Group siliciclastics, gold mineralization and local magnetics in the eastern area of the Taurus target. The hole intersected 0.13g/t Au over 27.43m (0.00-27.43), including 0.29g/t Au over 1.52m (7.62-9.14m). RAB drilling along with optical televiewer data analysis suggests mineralization is tied to intervals of dense oxidized fractures within the Carmacks Group andesite. Larger zones of pervasive oxidation outside of veining and fractures (see Photo 5) show increased sulphide content, but do not appear to host selectively elevated gold mineralization. Due to the inherent difficulty to determine geological and structural controls on mineralization, diamond drilling would be necessary to definitively confirm this relationship between the gold mineralization and the Carmacks Group. Though zones of oxidized fractures which occur in the hornblende diorite below 21.65m do produce sparse elevated gold assay values, the restriction of gold values to isolated oxidized structures along with the lack of width of these elevated zones supports the idea that gold mineralization is correlated with the siliciclastic Carmacks group, with mineralization tied to structures funneling fluids from overlying Carmacks siliciclastic strata. A cross section is provided in Figure 18 below which shows the grades intersected in hole WLFTRS23RAB001.

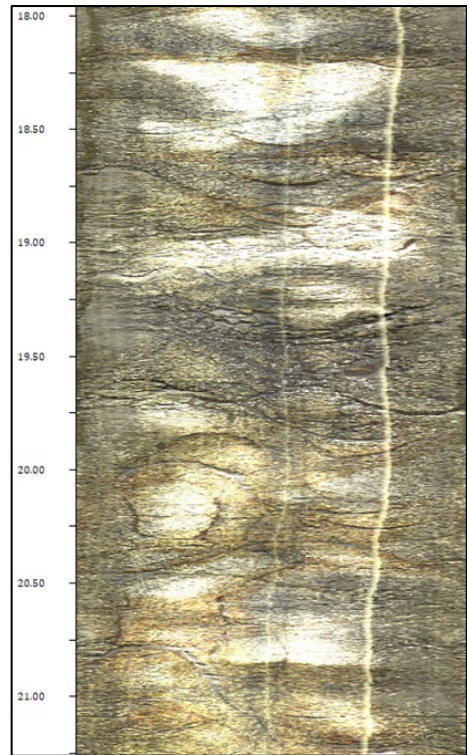
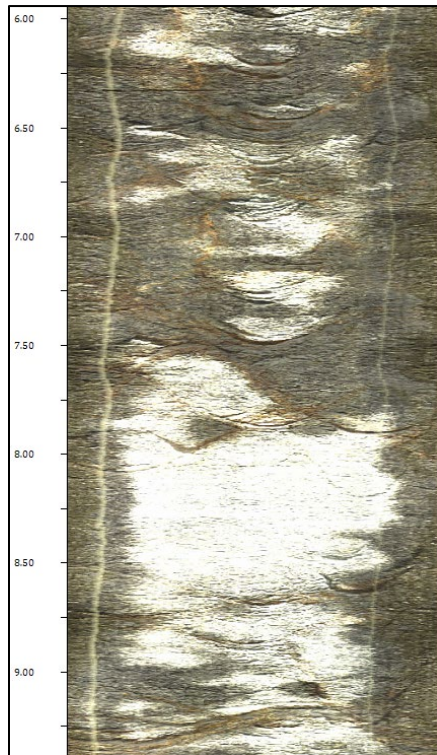


Photo 5. RAB Chip tray for WLFTRS23RAB0010.0-30.5m with oxidized andesite interval (45-75ft).

Photo 6. WLFTRS23RAB001 OTV image of oxidized fractures and patchy alteration 6.00-9.65m

Photo 7. WLFTRS23RAB001 OTV image of oxidized fractures as host of au-mineralization 18.00-21.50m



Photo 8. WLFTRS23RAB002 Chips showing mineralized and oxidized intervals (0.0-30.5m).

WLFTRS23RAB002 tested the strongest gold results from the 2017 GT Probe survey (Figure 9), a sub-vertical conductive feature identified in a 2017 IP line survey directly underneath the peak GT Probe gold values (Figure 10), and the apparent sharp contact between the magnetic low and high (figure 11). The hole intersected the most significant zone with 0.61g/t Au over 10.67m (18.29-28.9m), including 2.51g/t Au over 1.52m (18.29-19.81m), within a broader zone of 0.32g/t Au over 30.47m (13.72-44.19). Optical televiewer analysis revealed persistent intervals of strongly oxidized fracturing throughout the hole. Contrary to the oxidation-gold mineralization relationship seen in WLFTRS23RAB001, oxidation in WLFTRS23RAB002 becomes most dense before and after mineralized intervals., especially at 27.50-31.00m following the 18.29-28.96m mineralized interval hosting 0.61g/t Au over 10.67m. With this in mind, there appeared to be no overtly clear choice during WellCAD feature picking for the host of gold mineralization. The likely candidates are oxidized fractures similar to those found in WLFTRS23RAB001, though the hole’s oxidation profile varies considerably from WLFTRS23RAB002. Orientation of the candidate structures in both holes are 085-100°/45° (30-60° with outliers). A cross section is provided in Figure 18 below which shows the grades intersected in hole WLFTRS23RAB002.

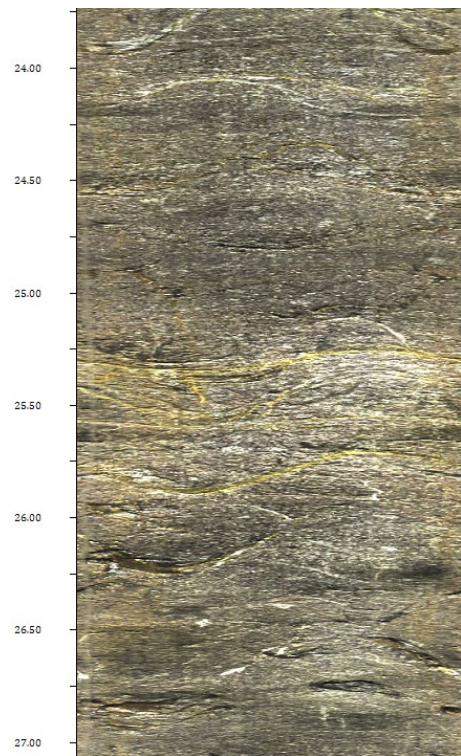


Photo 9. WLFTRS23RAB002 Oxidized Au-bearing fractures within unoxidized Carmacks andesite. Peak assay value of 0.715g/t Au at 24.4-25.9m

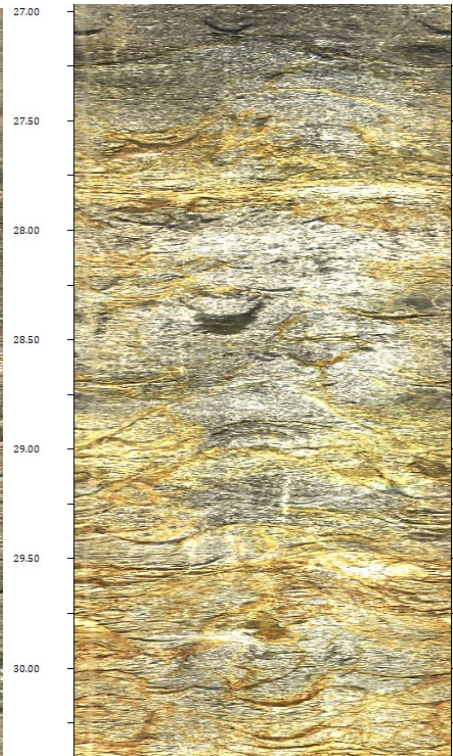


Photo 10. WLFTRS23RAB002 27.00-30.00m Sharp drop-off in Au mineralization to <0.2g/t occurs as oxidation density increases.

































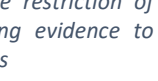
0.0 - 1.52m		30.48 - 32.00	
1.52 - 3.05m		32.00 - 33.53	
3.05 - 4.57m		33.53 - 35.05	
4.57 - 6.10m		35.05 - 36.58	
6.10 - 7.62m		36.58 - 38.10	
7.62 - 9.14m		38.10 - 39.62	
9.14 - 10.67m		39.62 - 41.15	
10.67 - 12.19m		41.15 - 42.67	
12.19 - 13.72m		42.67 - 44.20	
13.72 - 15.24m		44.20 - 45.72	
15.24 - 16.76m		45.72 - 47.24	
16.76 - 18.29m		47.24 - 48.77	
18.29 - 19.81m		48.77 - 50.29	
19.81 - 21.34m		50.29 - 51.82	
21.34 - 22.86m		51.82 - 53.34	
22.86 - 24.38m		53.34 - 54.86	
24.38 - 25.91m		54.86 - 56.39	
25.91 - 27.43m		56.39 - 57.91	
27.43 - 28.96m		57.91 - 59.44	
28.96 - 30.48m		59.44 - 60.96	

Photo 12. WLFTRS23RAB003 Chip Trays. Notice the restriction of pervasive oxidation to the upper 10ft (3m), Adding evidence to mineralization be restricted to tight oxidized structures

WLFTRS23RAB003 tested the gold anomaly outlined in GT Probe and soil sampling in the central area of the Taurus target associated with a magnetic low (Figure 10). The hole produced the greatest single sample interval outlier of the program with 6.55g/t Au, 37.38ppm Mo over 1.52m (21.34-22.86m), within a broader zone of 0.81g/t over 15.24m (19.81-35.05m). Also intersected was 0.14g/t Au over 21.33m (71.63-92.96m), including 0.18g/t Au over 3.05m (77.72-80.77m). WellCAD optical televiewer analysis of the isolated 6.55g/t Au interval at 21.34-22.86m suggests the mineralization is hosted in the fault structure at 22.75m (Photo 12). Though initial logged as diorite, visual and geochemical investigations suggest the majority of RAB003 is alkali basalt (Figure 20).

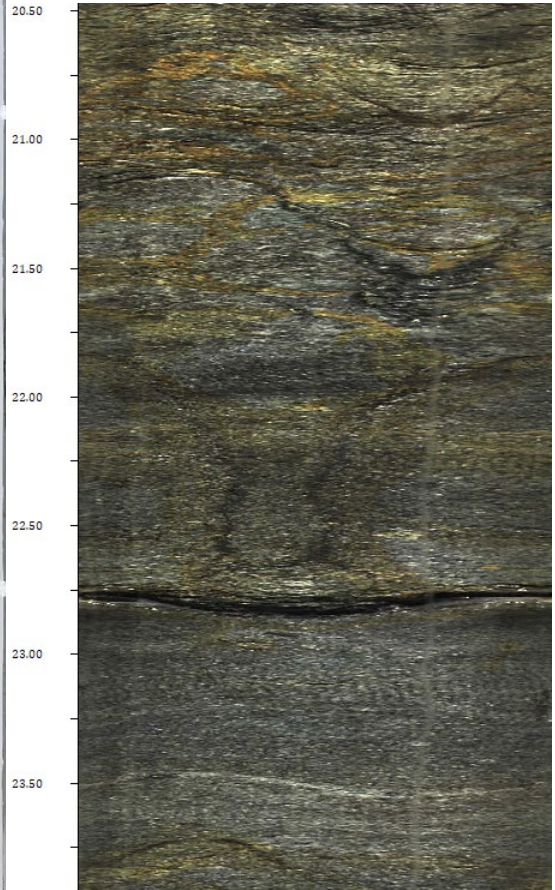


Photo 11. Mineralized Fault within non-oxidized Carmacks andesite. Peak Au value of 6.55g/t Au at 21.34-22.86m.















































0.0 - 1.52m		30.48 – 32.00m		<p>Groundwater was encountered at 22.86-24.34m during drilling suggesting the fault structure is part of a larger fluid system, accounting for the abnormal 6.55g/t Au spike. Though oxidation persists as defined oxidized structures sporadically distributed throughout the drill hole, there is a lack of patchy/pervasive oxidation intervals as encountered in holes 001 and 002 beyond the surficial oxidation down to 3m depth.</p> <p>WLFTRS23RAB004 tested the same structures and gold anomaly as WLFTRS23RAB003, from the opposite orientation of 000/-50°. The hole intersected 0.19g/t Au 0.27g/t Ag over 70.10m (0.00-70.10m), including 3.05g/t Au, 0.41g/t Ag over 3.05m (0.00-3.05m) and 0.29g/t Au 0.32g/t Ag over 7.62m (62.48-70.10m). Due to the collapse of the drill hole, no optical televiewer survey data was retrieved, limiting the structural interpretation of the hole. Surprisingly, RAB004 differs strongly from RAB003, which it scissors, both in alteration and mineralization extent.</p>
1.52 - 3.05m		32.00 – 33.53m		
3.05 - 4.57m		33.53 - 35.05m		
4.57 - 6.10m		35.05 – 36.58m		
6.10 - 7.62m		36.58 – 38.10m		
7.62 - 9.14m		38.10 – 39.62m		
9.14 - 10.67m		39.62 – 41.15m		
10.67 - 12.19m		41.15 – 42.67m		
12.19 - 13.72m		42.67 – 44.20m		
13.72 - 15.24m		44.20 – 45.72m		
15.24 - 16.76m		45.72 – 47.24m		
16.76 - 18.29m		47.24 – 48.77m		
18.29 - 19.81m		48.77 – 50.29m		
19.81 - 21.34m		50.29 – 51.82m		
21.34 - 22.86m		51.82 – 53.34m		
22.86 - 24.38m		53.34 – 54.86m		
24.38 - 25.91m		54.86 – 56.39m		
25.91 - 27.43m		56.39 – 57.91m		
27.43 - 28.96m		57.91 – 59.44m		
28.96 - 30.48m		59.44 – 60.96m		
				
				
				
				
				
				

Photo 13. WLFTRS23RAB004 Chip Trays. Note the comparison with WLFTRS23RAB003 chip trays in photo 12, which was drilled nearby in the opposite azimuth. Oxidation is significantly widespread, as is the persistent low Au values of 0.19g/t Au over entirety of the hole (0.0-70.10m (0-230ft)).

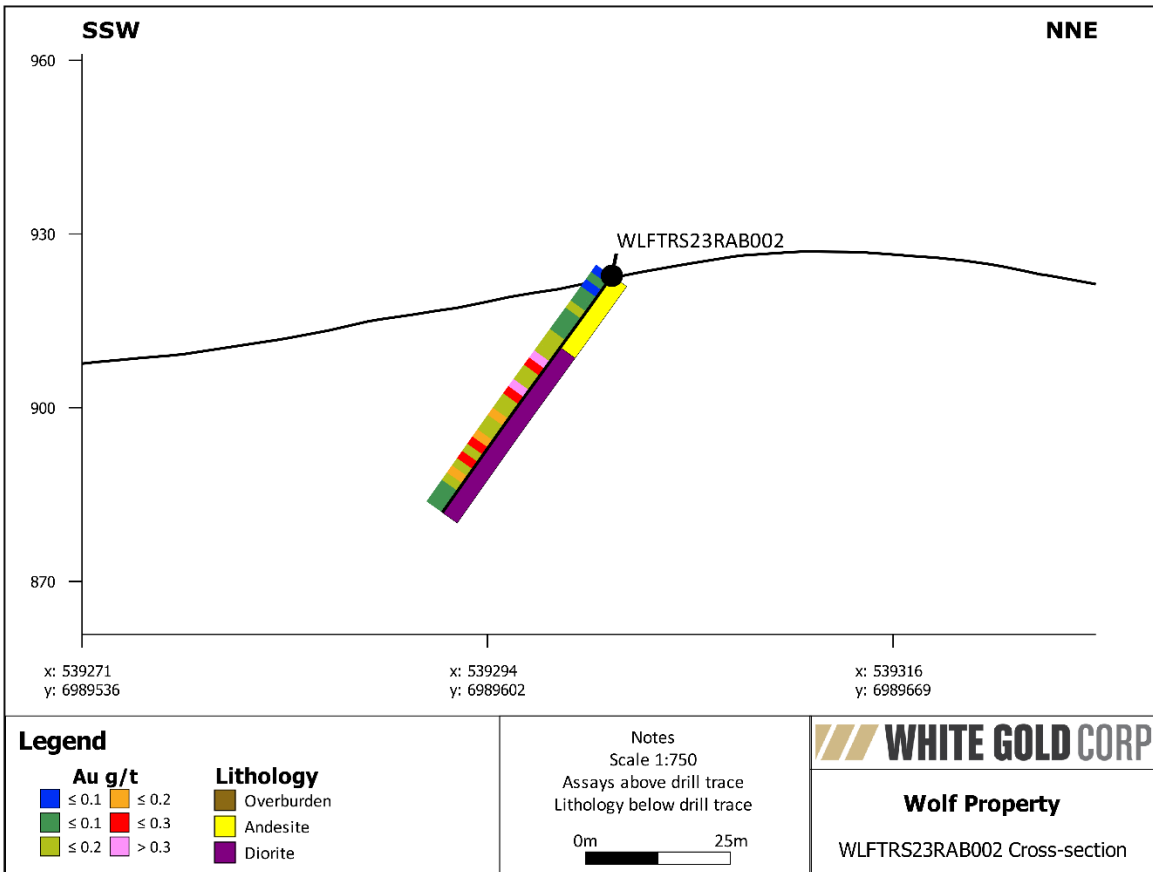
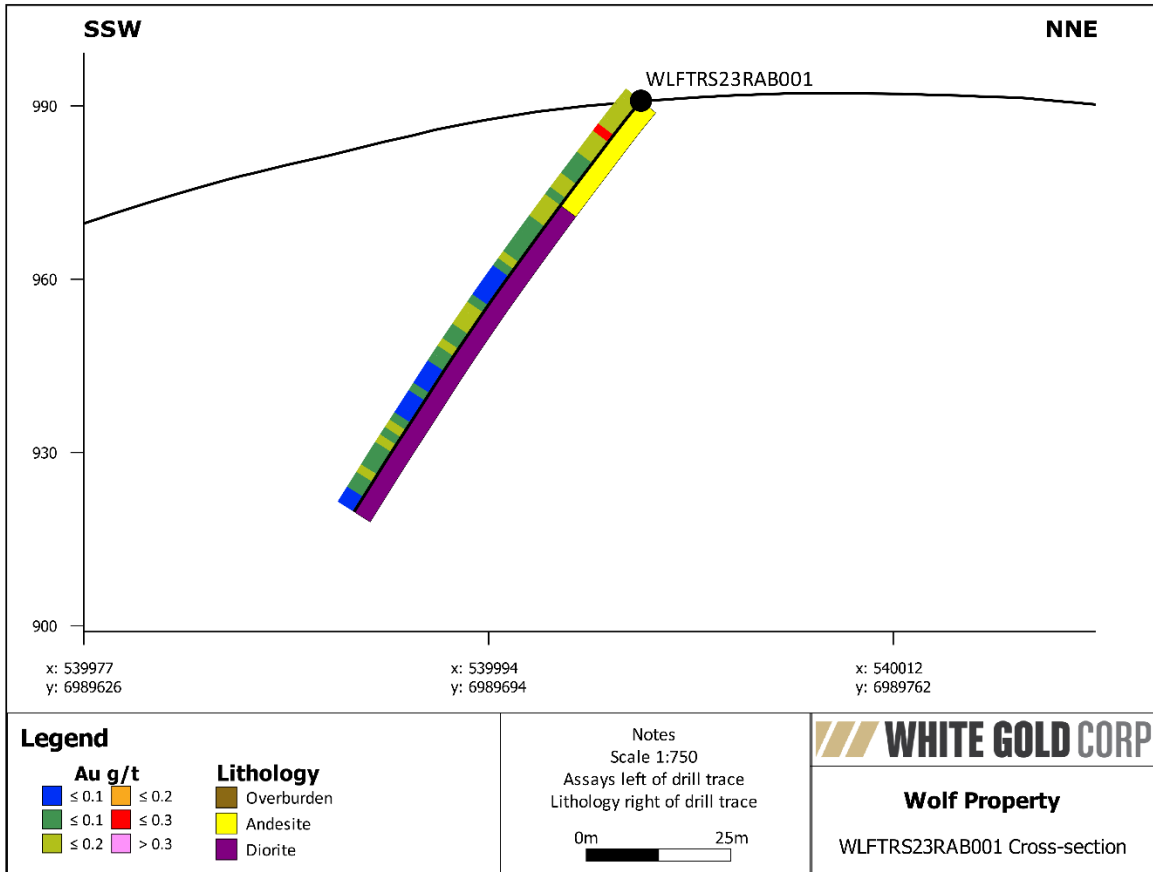


Figure 18. Cross-sections of RAB holes 001 and 002 showing lithology and gold assays in ppm

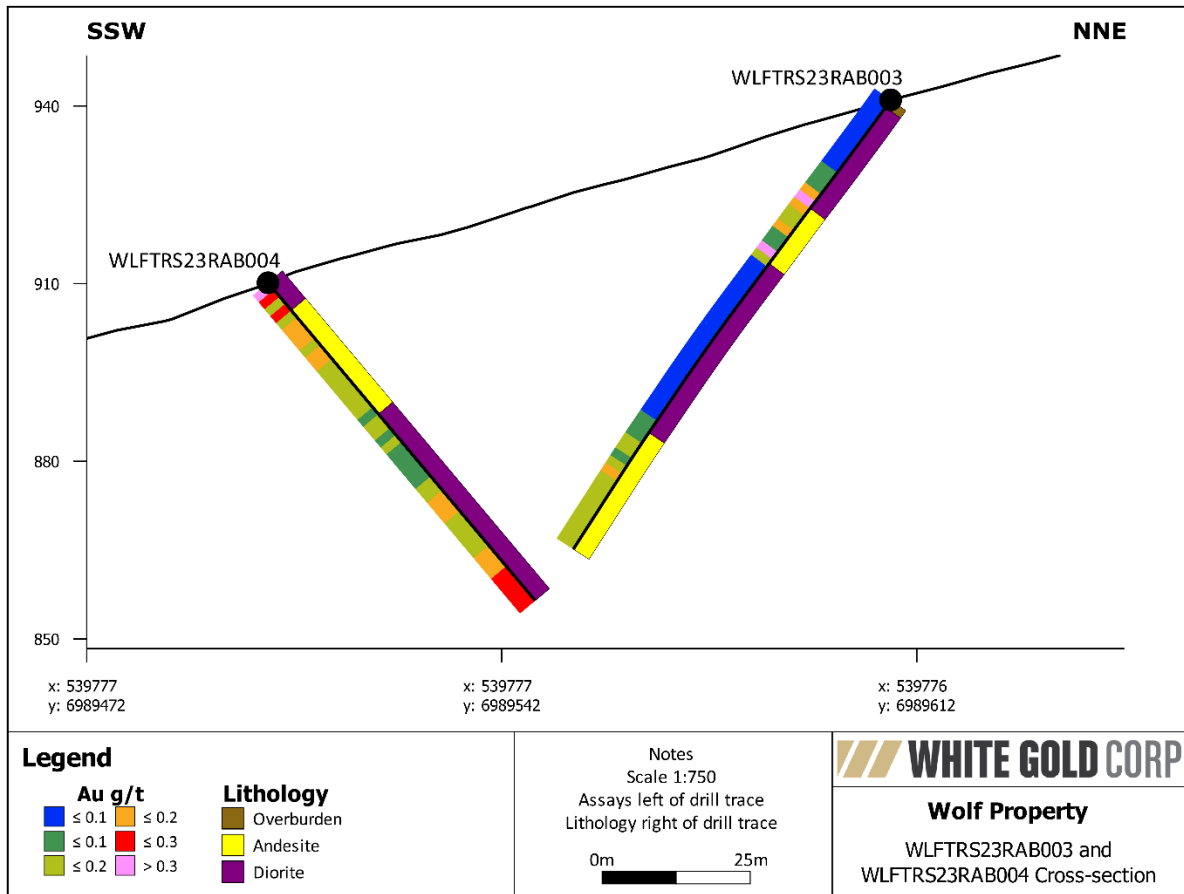


Figure 19. Cross-section of RAB holes 003 and 004 showing lithology paired with gold assays in ppm

Given the inherent difficulties of accurately identifying rock lithologies from RAB chip logging, assay results were analyzed in ioGAS™ using Pearce’s (1996) volcanic rock classification chart (Figure 20 and Figure 21), the Alumina Saturation in Igneous Rocks chart from Barton and Young (2002) (Figure 22), and the Tectonic Classification of Mafic Igneous Rocks by Cabanis and Lecolle (1989).

The Pearce (1996) figures utilize the immobile element ratios of Zr/Ti vs. Nb/Y to classify volcanic lithologies based upon differentiation rates of the immobile elements during magma evolution. This figure was used to assist interpretation of potential gold source and preferentially deposition lithologies.

The Barton and Young Alumina Saturation chart was initially created to classify magmatic-source non-pegmatitic beryllium deposits and occurrences by placing them in one of four groupings: Peralkaline, weakly peraluminous, strongly peraluminous, and metaluminous. This was done due to the lack of accounting for variation in alumina saturation (a_{Al2O3}) or silica saturation (a_{SiO2}), which are variables that “strongly influence Be and alteration mineral stability” (Barton and Young, 2002). For this report, the alumina saturation often directly reflects the magmatic source of igneous lithologies. As seen in Figure 22 below, the lithologies encountered during 2023 RAB drilling are predominantly weakly peraluminous to metaluminous.

The Tectonic Classification ternary plot from Cabanis and Lecolle (1989) uses ratios of the immobile elements Zr, Y, and Nb to classify igneous rocks as volcanic-arc basalts, continental basalts, and oceanic basalts. The large majority of RAB samples plot as calc-alkaline sourced rocks. Outliers plotting as late- to post-orogenic intra-continental produced anomalously high values of high field strength elements (HFSE), specifically Zr, Nb, and Th. Inspection of optical televiewer imagery shows no visual indications as to why

the outliers plot outside the main calc-alkaline group. This, along with the occurrence of fine oxidized structures, suggests post-deposition alteration as the cause for the outliers (See Photo 7 18.25-19.75m for example of outlier interval). All but one of these outliers produce elevated gold values (0.113-0.250 g/t Au). Unfortunately, four of the seven outliers appear in RAB004, from which televiewer data could not be retrieved, limiting interpretation of the outlier source.

Based on the analysis of the charts below, the primary lithologies encountered during the 2023 RAB drill program consisted of metaluminous to weakly peraluminous alkali basalts, andesites, and trachy andesites (Figure 20 and Figure 21). The bulk of anomalous gold values are concentrated within the basalt to alkali basalt compositions, though there are several >0.23g/t Au values found in the more intermediate and evolved regions (trachy andesite, andesitic basalt, trachyte, and rhyolite dacite). The evolved RAB samples occur exclusively in RAB004 within the interval of 4.57-27.43m depth. This interval is highly altered via oxidation, supporting the hypothesis that the outliers represent post-depositional alteration.

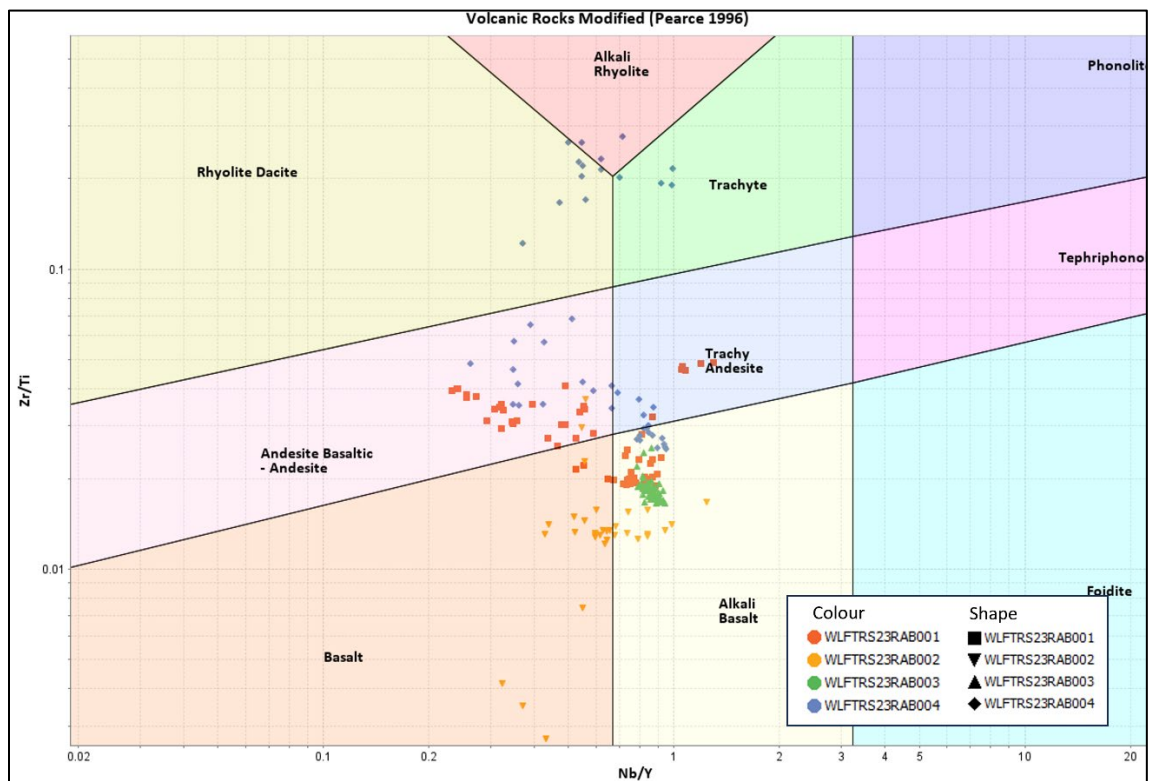


Figure 20. Volcanic Rock classification chart using immobile elements as proxy for TAS diagram (Pearce, 1996) showing distribution of the 2023 RAB hole samples.

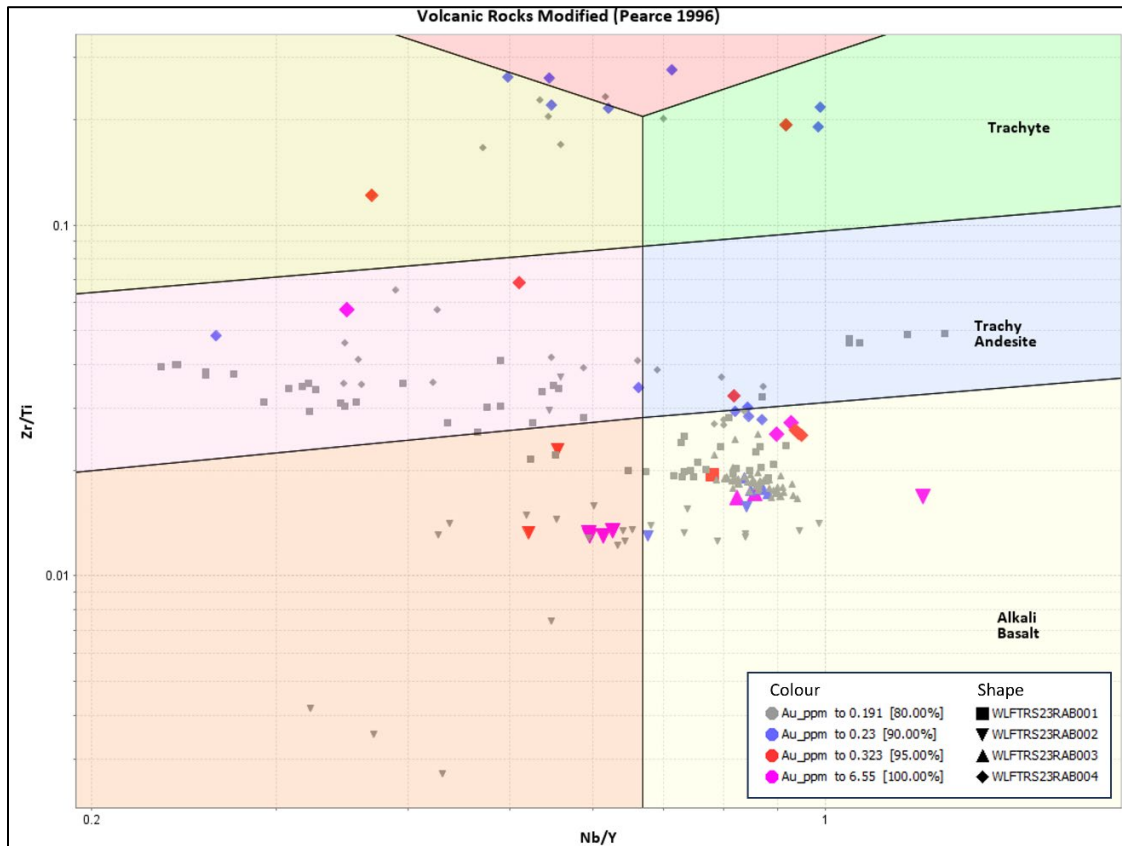


Figure 21. Modified figure 18 separating gold grade percentiles by colour. Note the preference of the 95th and 100th percentile, in red and purple respectively, for the basalt and alkali basalt regions.

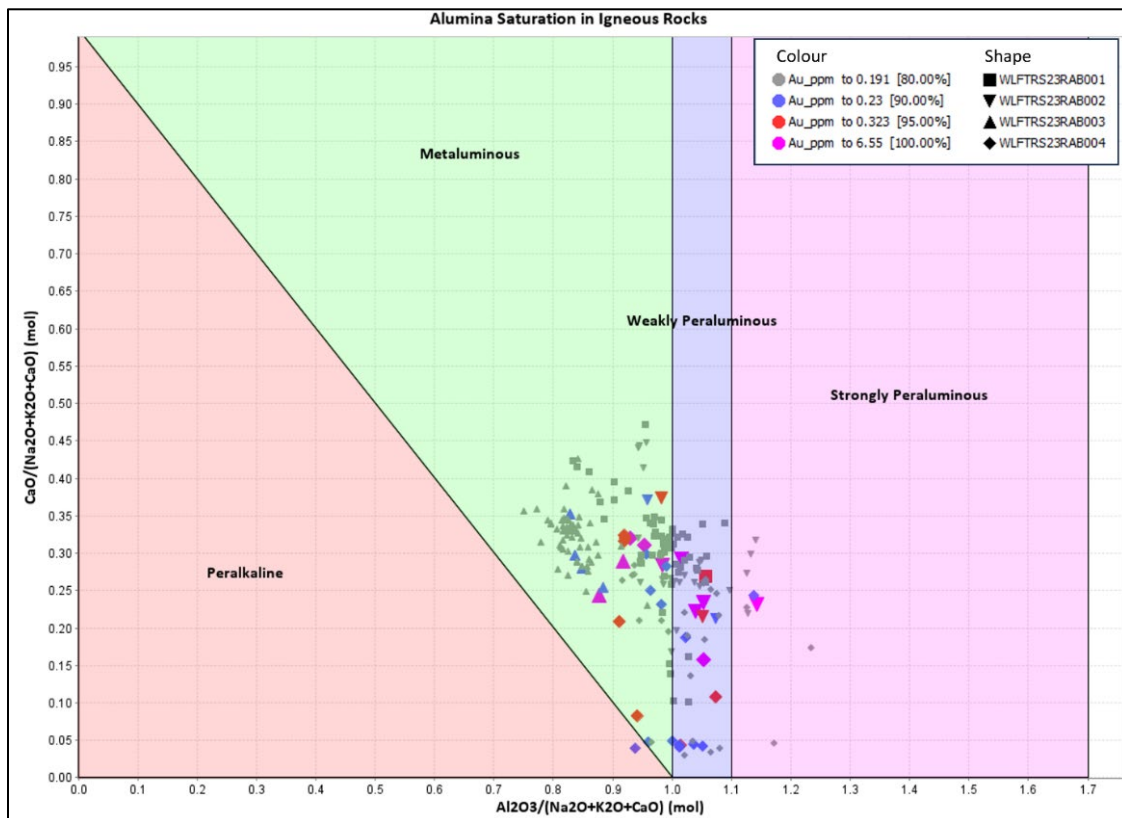


Figure 22. Alumina Saturation in Igneous Rocks (Barton and Young, 2002)

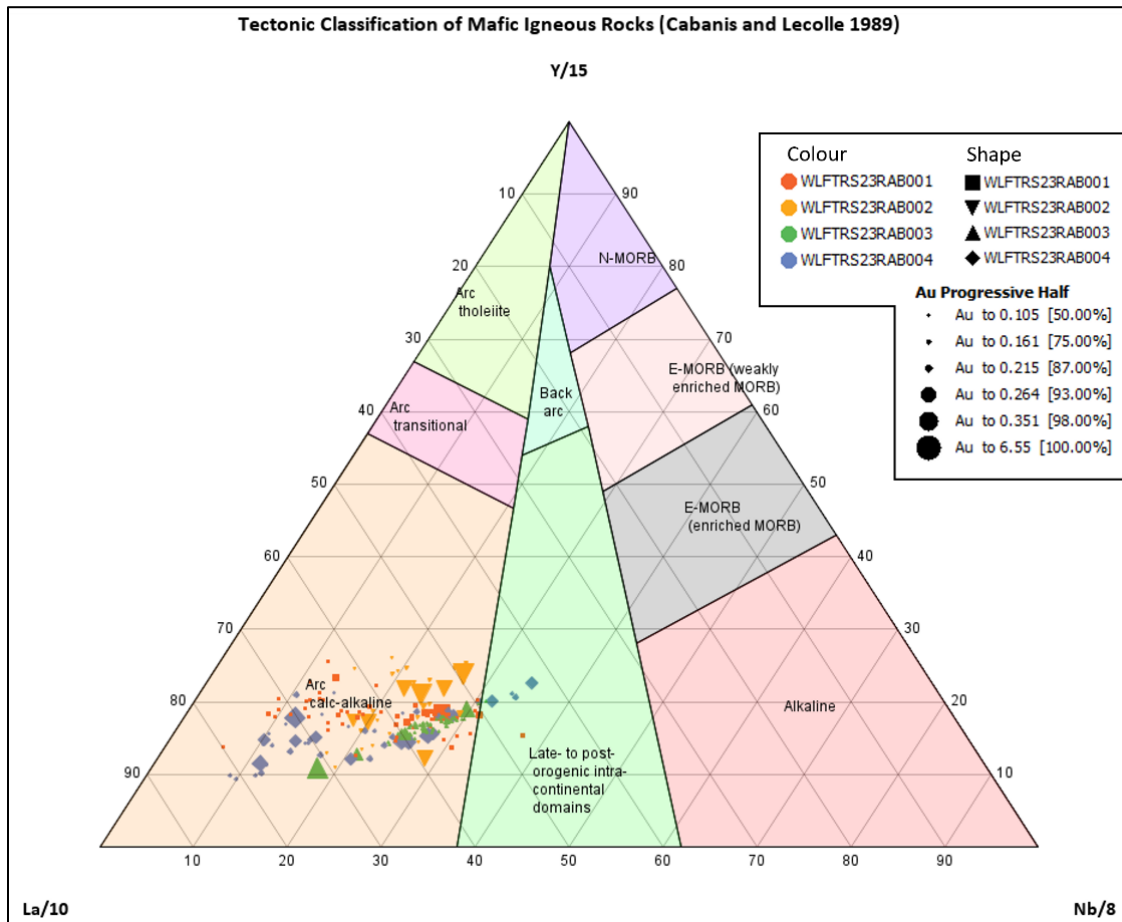


Figure 23. Tectonic classification of mafic igneous rocks showing a distinction between rocks encountered on the Taurus target during the 2023 RAB drilling program.

7.0 INTERPRETATION AND CONCLUSIONS

The Late Cretaceous Carmacks Volcanics Group have long been known as prospective hosts of several porphyry-style surface geochemical anomalies across the White Gold District, including White Gold’s Heart target (Nolan), X-Man target (JPR), and the Deuce target (Toonie, RAB drilled in 2023). Other intrusion-related and contemporaneous polymetallic vein occurrences within the district include the Bluff/Taurus Cu-Mo-Au porphyry (Early-Late Cretaceous, Eastern Alaska), The Pika target (Late Cretaceous, Eastern Alaska), Mt. Cockfield Cu-Mo, and the Swede and Pluto Mo-(Cu) prospects (North of Dawson). White Gold’s Taurus target lies within a thick sequence of these volcanics which have now been confirmed to extend from surface down to a minimum of up to 93m depth, based upon 2023 RAB drilling.

Intercepted lithologies included basalt and andesite (Figure 18 and Figure 19). Sections of increased oxidation within the Carmacks Group andesite tend to correlate to elevations in gold grades in assay results. The appearance of elevated gold assays along oxidized structures and lithological contacts outside the andesite initially suggested involvement of hydrothermal fluid facilitated endowment, possibly from a diatreme. Further investigation utilizing iGAS revealed the affect of late alteration on the lithochemical signature of many gold-bearing intervals, specifically RAB004, whose volcanic classification show extreme variation in comparison to RAB003 which scissored it (drilled in opposite

orientation and collared approximately 100m apart N-S). This geochemical variability between holes makes it difficult to confidently state that any one alteration is consistently associated with mineralization across the target area. Due to this variability, coupled with the inherent limitations of RAB drilling, preferential focus needs to be applied to these geochemical relationships.

The lithologies of the Carmacks Volcanic Group have a well researched and distinct geochemical signature that can be used to identify subtle variations in the alteration and lithological characteristics of the rocks intersected in the 2023 program. “All the lavas of the Carmacks Group are highly potassic” and “All the Carmacks lavas have a strong shoshonitic trace element signature, including enrichment in large ion lithophile elements (LILEs, e.g., K, Rb, Ba) and light rare earth elements (LREEs), but are relatively depleted in high field strength elements (HFS) (e.g., Nb, Zr, Ti).” (Johnson et al., 1996). Accordingly, any divergences from these trends likely signifies the involvement of post-depositional hydrothermal alteration, veining, or intrusions. The Carmacks’ distinct characteristics prove prospective as several shoshonitic and high-potassium calc-alkaline magmatic suites are associated with world-class hydrothermal gold and copper-gold mineralization. Examples include Oyu Tolgoi, Mongolia and Bingham, Utah copper-gold mines”.

Initial interpretation appeared to show mineralization differentiated between hole 001 and 002 with respect to the oxidation style (fractures vs frac+halo/flooding). Further study of the structures suggest that mineralization is indeed concentrated in the oxidized fractures. Hole 002 hosts extensive strongly altered and oxidized intervals surrounding mineralized fractures that do not present elevated gold values. This suggests the alteration is a by-product of the oxidizing fluid conduits, but as a non-auriferous generation of fluid flow, restricting gold mineralization exclusively to the oxidized fractures themselves (Photo 14). The concentration of gold mineralization in WLFTRS23RAB002 along the middle section of the planned hole, corresponds with the magnetic low field shown in Figure 10. This supports the use of magnetic lows as part of a vectoring package for further exploration of the property.

RAB004 provided the most consistent and extensive elevated gold values. It also produced the most anomalous values both in regards to lithological source (Figure 20 and Figure 21) and melt source (Figure 23). Whereas RAB003 was collared into, and drilled entirely within a magnetic high, RAB004 was drilled in the opposite orientation, collaring in a magnetic low and drilling across the low/high magnetic interface. Could this interface represent a gold feeder structure like that projected in Figure 10?

It is the opinion of the author of this report that RAB004 represents a well altered/oxidized structural corridor, focusing gold mineralization sourced from late andesitic Carmacks intrusives, into underlying Carmacks group basalts along pre- and syn-depositional structures. The lack of consistent width or grade in the gold zones of RAB hole 001, 002, and 003 are concluded to be the result of mineralization being strongly isolated to fine to medium-fine oxidized fractures. The fact they are so well oxidized suggests their status as long-lived open structures permitting long-term fluid cycling, increasing the potential for gold-bearing solutions to deposit gold. This makes the magnetic low-high interface intersected by RAB004 the primary candidate for diamond drill on the Taurus target. The secondary candidate would be the intersection of Carmack siliciclastic with basalts seen in RAB002, which produced good results, hosting its greatest value at the top of the interval, suggesting a contact or structure-focussed mineralization, followed by deeper distribution along underlying fractures/structures.

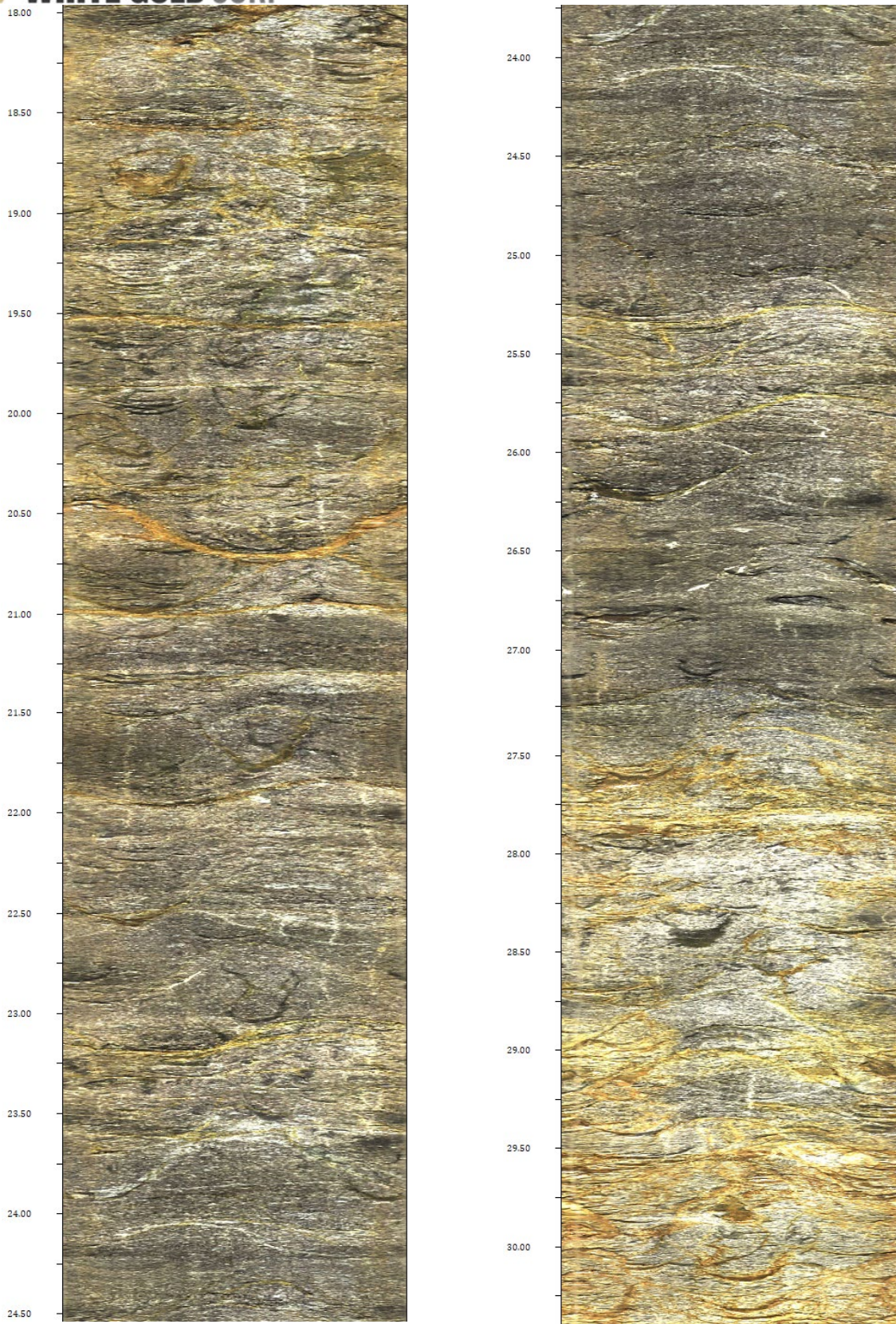


Photo 14. WLFTRS23RAB002 OTV Images showing variability of oxidation alteration in relation to mineralization. Note that oxidized structures at 18.00-19.50m (upper left column) are mineralized with 2.51g/t Au whereas the more oxidized region at 27.50-30.65m (lower right column) are restricted to < 0.25g/t Au. This suggests that mineralization is tied to the structures and not extensive penetrating oxidation into surrounding wall rock

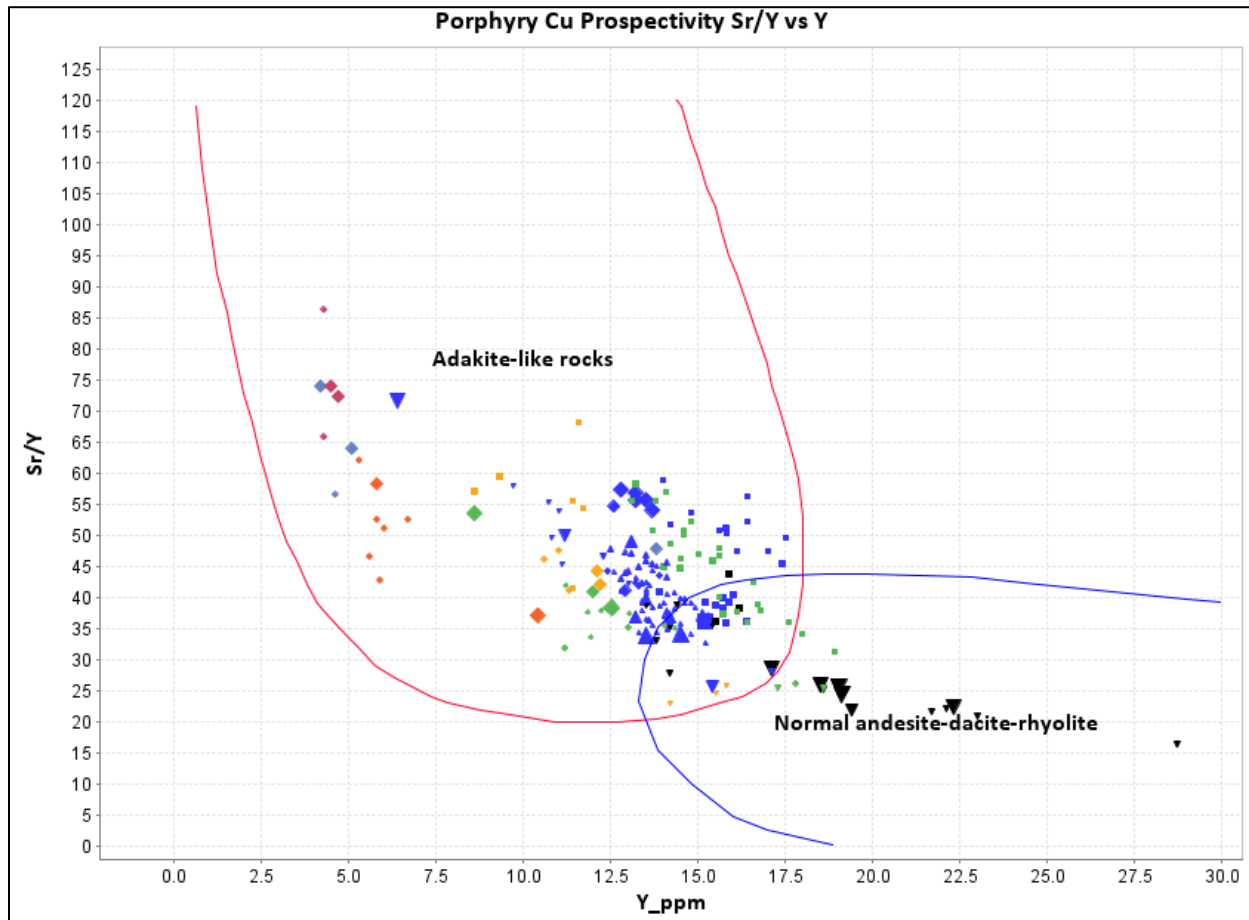


Figure 24. Porphyry prospectivity diagram showing RAB samples which do not plot as Basalt carry a geochemical signature similar to adakite-like rock. Note that adakite-like clusters tend to carry Cu-Au mineralization (Richards et al., 2012)

8.0 RECOMENDATIONS

The 2023 RAB drill program produced interesting results, both positive and negative. While gold mineralization is not consistent across the holes, it does show promise in specific areas (RAB002 and RAB004). As such, it is recommended that future work be focused on explaining the grade variability between RAB003 and RAB004, along with the influence of the magnetic low-high transition of future exploration vectoring. To accomplish this, a modest diamond drill program of three to four holes should be completed, with two holes intersecting the magnetic transition and one to two holes targeting the auriferous structure intercepted in RAB002.

With the influence of alteration having an critical influence in certain locals (RAB004, mineralized fractures), alteration mapping with SWIR analysis should be utilized to identify the correct alteration profile for future target generation before extensive diamond drilling programs are designed. Additional field mapping could be helpful in this endeavour through increased detail and field sample collection to help eliminate exposure alteration from desired alteration profiles.

9.0 REFERENCES

- Allan, M. et.al., 2012. Metallogenic Framework for Lode Gold in the White Gold and Dawson Range Districts, Yukon Geoscience Forum 2012.
- Banys, Vytas., Crawford, Kaitlyn., 2019. Geochemical Assessment Report (Soil sampling, Prospecting, GT Probe) on the Wolf Property. Dawson Range. Yukon.
- Barton, M.D. and Young, S., 2002, Non-pegmatitic deposits of beryllium: mineralogy, geology, phase equilibria and origin in E.S. Grew, ed., Beryllium: Mineralogy, Petrology and Geochemistry: Reviews in Mineralogy and Geochemistry, v. 50, p. 591-691.
- Cabanis, B. and Lecolle, M., 1989, The La/10-Y/15-Nb/8 diagram: A tool for distinguishing volcanic series and discovering crustal mixing and/or contamination: Comptes Rendus de l'Academie des Sciences, Serie 2, Sciences de la Terre, 309, 20p.
- Cooley, Michael., 2017. Preliminary Geologic Map of the Wolf Target Area, White Gold District, Yukon. Internal report.
- Fage, Adam., Hanlon, Jen., Radjaee, Amir., 2018. Geochemical, Geophysical, and Airborne Survey Assessment Report. Wolf Gold Project.
- Jilson, G., and Brownlee, D.J., 2000. Geochemical and Geological Report on the Au and P Claims. Deltango Gold Ltd., Yukon assessment Report #094173.
- Pautler, J., 2011. Technical Report on the Wolf and Betty Properties, Dawson Range, Yukon Territory. Ethos Capital Corp., by J.P. Exploration Services inc., (available at www.sedar.com).
- Pearce, J.A., 1996. A user's guide to basalt discrimination diagrams. In: Wyman, D. A. (ed.) Trace Element Geochemistry of Volcanic Rocks: Applications for Massive Sulphide Exploration. Geological Association of Canada, Short Course Notes 12, 79 to 113.
- Richards et al., 2012, High Sr/Y Magmas Reflect Arc Maturity, High Magmatic Water Content, and Porphyry Cu +/- Mo +/- Au Potential: Examples from the Tethyan Arcs of Central and Eastern Iran and Western Pakistan, Economic Geology, v.107, pp. 310, Fig 9c
- Ryan, Shawn., 1998. Report for Grass Root Prospecting. YMIP #98-044.
- Ryan, Shawn., 2008. Geochemical Report Cu 1-8 Claims Grant # YC00871-YC00878. Yukon Assessment Report #094074.
- Ryan, Shawn., 2010. Geochemical / Geophysical Report Wolf 1-42 claims Grant #YC83707-YC83747. Whitehorse Mining District. Yukon. Assessment Report # 095239.
- Tallman, Peter., 2012. Prospecting, Soil Geochemistry, Airborne Magnetic and Radiometric Surveying, and Airphoto-Orthophoto Surveying on the Wolf Project, White gold District. Yukon Territory. Ethos Gold. Assessment Report # 096157.

Watson, R.K., 1971. Report on an Airborne magnetic Survey Libra Claims, White River Area for Marguerite Lake Mines. Whitehorse Mining District. Yukon Territory. Assessment Report # 060244.

10.0 STATEMENT OF EXPENSES

A total of \$199,254.63 was spent on the 2032 Wolf RAB filed exploration program. Of these expenditures, \$160,273.72 are expected to qualify as eligible “Target Evaluation” cost incursions for Yukon Mineral Exploration Program (YMEP) funding. A summary of expenditures is shown in Table 11 below.

2023 Wolf Expenditure Summary	WLF Project Total	YMEP Eligible Expenses
1.1: RAB Drilling Production	78,855.63	54,409.85
1.2: Assays and Shipping	11,242.06	11,242.06
1.3: Helicopter, Transport, fuel	82,779.84	82,779.84
1.4: Crew Travel	6,832.80	0.00
1.0: RAB Drilling - Groundtruth Drilling, GroundTruth Exploration, Bureau Veritas, Great Slave Helicopters, Tintina Air	\$179,710.32	\$148,431.75
2.1: Pad Building Labour	9,569.25	2,500.00
2.2: Helicopter	6,043.37	6,043.37
2.3: Crew Travel/Mobilization	3,931.69	3,298.61
2.0 Pad Building - Minconsult Exploration Services, Great Slave Helicopters.	\$19,544.30	\$11,841.97
Total 2023 Wolf Expenditure	\$199,254.63	\$160,273.72
YMEP Claim Amount		\$50,000.00

Table 11. Summary of 2023 RAB Exploration Expenditures

11.0 STATEMENT OF QUALIFICATIONS

I, Steven Walsh, do hereby declare that:

1. I am currently assisting with end of season report writing for White Gold Corp.
2. I graduated from the University of Saskatchewan in 2012 with a B.Sc. (Hons) degree in Geology and Queen's University in 2015 with a M.Sc. in Geology.
3. I have worked as a geologist on and off since 2012, including as an Exploration Geologist for White Gold Corp since June 2023.
4. I am not aware of any material fact or material change with respect to the subject matter of this report, the omission to disclose which makes this misleading.

Dated this 15th day of December, 2023

Steven Walsh